Tuberculosis 147 (2024) 102493

Contents lists available at ScienceDirect

Tuberculosis

journal homepage: www.elsevier.com/locate/tube

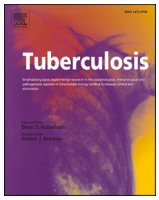

Caveolin-1 affects early mycobacterial infection and apoptosis in macrophages and mice

Yuqing Wu [a], Andrea Riehle [a], Barbara Pollmeier [a], Stephanie Kadow [a], Fabian Schumacher [b], Marek Drab [c], Burkhard Kleuser [b], Erich Gulbins [a], Heike Grassmé [a,*]

[a] Institute of Molecular Biology, University Hospital Essen, University of Duisburg-Essen, Hufelandstrasse 55, 45122, Essen, Germany
[b] Institute of Pharmacy, Freie Universität Berlin, Berlin, Germany
[c] Unit of Nanostructural Biointeractions, Department of Immunology of Infectious Diseases, Ludwik Hirszfeld Institute of Immunology and Experimental Therapy, Polish Academy of Sciences, 12 Weigla Street, 53-114, Wroclaw, Poland

ARTICLE INFO

Keywords:
Tuberculosis (TB)
Mycobacterium bovis Bacillus Calmette-Guérin (BCG)
Caveolin-1
Apoptosis
Ceramide
Cytokines
Macrophages

ABSTRACT

Tuberculosis, caused by *Mycobacterium tuberculosis*, remains one of the deadliest infections in humans. Because *Mycobacterium bovis* Bacillus Calmette-Guérin (BCG) share genetic similarities with *Mycobacterium tuberculosis*, it is often used as a model to elucidate the molecular mechanisms of more severe tuberculosis infection. Caveolin-1 has been implied in many physiological processes and diseases, but it's role in mycobacterial infections has barely been studied. We isolated macrophages from Wildtype or Caveolin-1 deficient mice and analyzed hallmarks of infection, such as internalization, induction of autophagy and apoptosis. For *in vivo* assays we intravenously injected mice with BCG and investigated tissues for bacterial load with colony-forming unit assays, bioactive lipids with mass spectrometry and changes of protein expressions by Western blotting. Our results revealed that Caveolin-1 was important for early killing of BCG infection *in vivo* and *in vitro*, controlled acid sphingomyelinase (Asm)-dependent ceramide formation, apoptosis and inflammatory cytokines upon infection with BCG. In accordance, Caveolin-1 deficient mice and macrophages showed higher bacterial burdens in the livers. The findings indicate that Caveolin-1 plays a role in infection of mice and murine macrophages with BCG, by controlling cellular apoptosis and inflammatory host response. These clues might be useful in the fight against tuberculosis.

1. Introduction

Tuberculosis, caused by *Mycobacterium tuberculosis*, remains one of the most serious global diseases affecting human, with nearly two million people dying annually [1,2]. Thus, even in recent years it is the deadliest infection in humans behind SARS-CoV-2-infection [3]. About one-third of the world's population has latent tuberculosis (TB) and 5–10% of people with latent TB will develop active disease sometimes during their lives underlining the high significance of this infection. Although Tb is predominantly a respiratory infection, extrapulmonary or disseminated *M. tuberculosis* infection may enhance the risk of latent infection, thereby impairing successful drug prophylaxis or medical treatment [4,5]. It is therefore important to understand the circumstances of mycobacterial dissemination and persistence in more detail. *Mycobacterium bovis* Bacillus Calmette-Guérin (BCG), a species belonging to the *Mycobacterium tuberculosis* complex, induces predominantly zoonotic diseases and is the main cause of bovine and deer tuberculosis [6]. It can also infect immune-incompetent humans, which have been in close contact with infected animals or their products. Human tuberculosis and zoonotic BCG infections have co-evolved with a similar disease profile and host immune response [6]. *Mycobacterium bovis* Bacillus Calmette-Guérin (BCG), the current vaccine strain against tuberculosis was attenuated by serial passages of virulent *Mycobacterium bovis*, which share >99% genetic identity to *Mycobacterium tuberculosis* [7]. Taken advantage of this, BCG is often used as a model to elucidate the molecular mechanisms of more severe tuberculosis.

Host macrophages and neutrophils of the innate immune system provide a first line of defense against *Mycobacterium tuberculosis* and BCG. Both pathogens are internalized by macrophages through phagocytosis and subsequently located within phagosomes, which undergo a series of fusion events to mature and achieve anti-microbial properties

* Corresponding author.
E-mail address: heike.gulbins@uk-essen.de (H. Grassmé).

https://doi.org/10.1016/j.tube.2024.102493
Received 16 October 2023; Received in revised form 9 February 2024; Accepted 11 February 2024
Available online 12 February 2024

[8,9]. This initial inflammatory response leads to the recruitment of neutrophils, monocytes, and further macrophages, which then differentiate into epithelioid cells, multinucleated giant cells and foamy macrophages, providing the basic components of granuloma, which is a hallmark of tuberculosis and generally known to promote the persistence of bacteria [10]. Mycobacteria are highly adapted to macrophages and have multiple mechanisms to resist the host immune responses [11]. Consequently, host innate immune mechanisms have co-evolved with the pathogen to better counter mycobacterial infections [12].

Caveolae form a subgroup of distinct membrane domains, often named lipid rafts, and stabilize and concentrate lipids, including cholesterol, sphingomyelin, glycosphingolipids, and the caveolin proteins [13–15]. Accordingly, caveolar functions are very diverse and range from cholesterol homeostasis, vesicular trafficking to signal transduction processes and cell death [16–18]. The main component of caveolae is Caveolin-1 (Cav-1), a small, 24 kDa integral membrane protein, associated with cell signaling cascades through direct interaction with multiple proteins such as Src family tyrosine kinases, endothelial NO synthase (eNOS) and the insulin receptor [19–21]. Stress-induced changes in rafts lead to altered receptor tyrosine kinase signal transduction through a modulation of Caveolin-1 by acid sphingomyelinase-derived ceramide [22]. Caveolin-1 has been also linked to cell death signaling pathways and apoptosis [23–27]. Recent studies demonstrate that Caveolin-1 expression negatively correlates with tumor cell apoptosis of different cell types [23,24] and that enhanced apoptosis sensitivity of Caveolin-1-deficient endothelial cells was linked to acid sphingomyelinase/ceramide signaling [27].

Caveolin-1-deficient mice show a complete ablation of morphologically identifiable caveolae in almost all cell-types examined and display higher bacterial burdens, decreased phagocytosis ability, higher production of inflammatory cytokines and increased mortality upon infection with *Pseudomonas aeruginosa* [28], *Salmonella enterica* serotype Typhimurium [29] and *Klebsiella pneumonia* [30]. Additionally, several studies have demonstrated, that bacteria and viruses, including echovirus [31], respiratory syncytial virus [32], Simian virus 40 [33], HIV-virus [34], *Salmonella enterica* serotype Typhimurium, and certain FimH-expressing bacteria [35] are internalized via a caveolae-mediated endocytic pathway. *In vitro* studies have demonstrated that lipid rafts play a crucial role in the entry of *Mycobacterium tuberculosis* [36], *Mycobacterium avium* [37] and *Mycobacterium kansasii* [38] in macrophages. Cholesterol depletion inhibits uptake of these microorganisms [39], which may in turn influence the course of infection. BCG infection of monocytic myeloid-derived suppressor cells (M-MDSCs), which are massively activated in TB patients, leads to an upregulation of Caveolin-1, which induces TLR2 signaling, required for T cell suppressor functions [40].

These few studies on mycobacteria and Caveolin-1 suggest an important role of Caveolin-1 for mycobacterial infections of macrophages; however, molecular details are unknown and require definition.

We therefore investigated whether infection of murine macrophages and mice with BCG is regulated by Caveolin-1. We examined internalization, hallmarks of signal transduction processes in phagocytosis, autophagy and apoptosis, inflammatory cytokines and involvement of sphingomyelinase/ceramide-system after BCG infection in Wt and Caveolin-1 deficient mice and macrophages. The sphingomyelinase/ceramide-system is also involved in the organization of membranes: Formation of ceramide upon sphingomyelin hydrolysis via sphingomyelinases leads to the formation of large lipid platforms domains, which serve to sequester proteins such as cell surface proteins in a dynamic membrane environment [41–43]. Further, ceramide-enriched membrane domains have been shown to be involved in infection of mammalian cells, for instance by *Pseudomonas aeruginosa*, *Staphylococcus aureus* and Rhinovirus [44–46]. It is therefore very interesting to study the interaction of caveolae and ceramide-enriched membrane domains during BCG infections.

Our findings revealed that internalization of BCG by macrophages was independent of Caveolin-1. Instead, Caveolin-1 was involved in killing of BCG early after in vivo and in vitro infection, and controlled acid sphingomyelinase (Asm)-dependent ceramide formation, apoptosis and inflammatory cytokines upon infection with BCG. In accordance, Caveolin-1 deficient mice displayed higher bacterial burdens in infected macrophages and livers of mice. These studies provide insights into the functional role of Caveolin-1 in BCG infection of murine macrophages.

2. Materials and methods

2.1. Mice and cells

C57BL/6JOlaHsd Wildtype (Wt) mice and Caveolin-1 (Cav-1) deficient mice (Cav1 ^{tm1Mls}/J, Cav1$^{-/-}$) were generated by Dr. Marek Drab [47] and kindly provided by Prof. Dr. Verena Jendrossek and Prof. Dr. Diana Klein from the Institute of Cell Biology, University of Duisburg-Essen. Mice were re-derived by embryo transfer prior to use in our animal facility to guarantee highest standards of a pathogen-free environment. All mice were housed under specific pathogen-free conditions in the animal facility at the University of Duisburg-Essen according to the criteria of the Federation of Laboratory Animal Science and used aged 6–12 weeks. The genotype was verified by polymerase chain reaction (PCR) analysis before experimentation. *In vivo* infections were approved by the Landesamt für Natur, Umwelt und Verbraucherschutz (LANUV), animal grant G 1691/18; permission number 81–02.04.2018. A192.

The *in vitro* experiments were performed with bone marrow-derived macrophages (BMDMs) obtained from Wt and respective knock-out mice. The culture of bone marrow-derived macrophages has been previously described in detail [48]. Briefly, mice were sacrificed, and femurs and tibias were flushed with minimum essential medium (MEM; Gibco, Paisley, UK) supplemented with 10% fetal bovine serum (Gibco), 10 mM HEPES (Roth GmbH, Karlsruhe, Germany; pH 7.4), 2 mM L-glutamine, 1 mM sodium pyruvate, 100 μM nonessential amino acids, 100 U/mL penicillin, and 100 μg/mL streptomycin (Gibco). Isolated cells were passed through a 23-G needle to obtain single cells, which were cultured for 24 h in small tissue-culture flasks. Cells were washed, and 3×10^4 or 1.2×10^5 non-adherent cells were cultured in 24- or 6-well plates in MEM with 20% L-cell supernatant as a source of macrophage colony-stimulating factor (M-CSF). Fresh MEM/L-cell supernatant medium was applied after 4 days of culture. Macrophages matured within the next 6 days and were used on day 10 of culture.

2.2. Infection experiments

All *in vivo* and *in vitro* infections were performed with green fluorescent protein (GFP)-expressing BCG (GFP-BCG) [49,50]; background is the BCG Vaccine SSI, BCG-Danish strain 1331. The GFP-BCG strain was constructed by transforming BCG with the dual reporter plasmid pSMT3L × EGFP [50]. For infection experiments, bacteria were gently shaken in Erlenmeyer flasks with 10 ml Middlebrook 7H9 Broth with Glycerol (BD Biosciences, Heidelberg, Germany), supplemented with 50 μg/mL Hygromycin B for maintaining GFP-plasmids. Bacteria were used for infection experiments after 5–7 days of culture. Bacteria were collected by centrifugation at 880×*g* for 10 min. The bacterial pellet was resuspended in HEPES/Saline buffer (H/S) consisting of 132 mM NaCl, 1 mM $CaCl_2$, 0.7 mM $MgCl_2$, 20 mM HEPES (pH 7.3), 5 mM KCl, and 0.8 mM $MgSO_4$ and was vortexed for 5 min. Samples were bath-sonicated for 5 min at 4 °C and were passed 10 times through a syringe with a needle 0.8 mm in diameter. Clumps of bacteria were removed by centrifugation for 2 min at 220×*g*. The supernatant containing single cells of GFP-BCG was carefully collected. The bacterial number was calculated by measuring the optical density and a standard curve prior to infection.

For *in vitro* assays, bone marrow-derived macrophages were left uninfected or infected with GFP-BCG in MEM/10 mM HEPES at a

bacteria-to-host cell ratio (multiplicity of infection, MOI) of 10:1 to 50:1. Synchronous infection conditions and enhanced interactions between bacteria and host cells were achieved by 8-min centrifugation (55×*g*) of the bacteria onto the cells. The end of the centrifugation was defined as the starting point of infection. The infection was terminated by fixation or lysis, as described below. For *in vivo* infections, bacteria were prepared as above and then pelleted at 2240×*g* for 10 min. BCG were resuspended in 0.9% NaCl, and 1×10^7 bacteria in 100 μL were intravenously injected into mice. After the indicated time, the animals were sacrificed by cervical dislocation. Serum was taken, respectively, livers were removed for further processing.

2.3. Quantification of colony-forming units

To quantify BCG colony-forming units (CFU) in tissues, we removed the livers and spleens from infected mice, added 5 mg/mL saponin (Serva Electrophoresis GmbH, Heidelberg, Germany) in H/S to lyse mammalian cells, but not the bacteria, and homogenized the tissues in a loose Dounce homogenizer (Braun, Kronberg, Germany). The homogenates were incubated for 30 min at 37 °C on a thermomixer for the release of intracellular bacteria. Samples were centrifuged for 2 min at 220×*g* and resuspended in PBS. Supernatants were diluted in PBS and plated on Middlebrook 7H10 agar supplemented with oleic acid (OADC) (BD Biosciences, Heidelberg, Germany). For colony forming unit (CFU) assays with bone marrow-derived macrophages, infected cells were washed once with MEM/10 mM HEPES after indicated infection times to remove non-adherent bacteria and were then lysed in 3 mg/mL saponin for 30 min at 37 °C to release intracellular bacteria. We plated 100-μL aliquots and counted bacterial CFU, after an incubation time for approximately 2 weeks in a humidified 37°C atmosphere.

2.4. Assay for neutral and acid sphingomyelinase activity

Acid and neutral sphingomyelinase activities were determined as recently described [51] with green-fluorescent BODIPY FL C_{12}-sphingomyelin (Thermo Fisher Scientific, Waltham, MA, USA) as a substrate. Briefly, cells were infected or left untreated, harvested and lysed in 250 mM sodium acetate (Sigma) with 1% Nonidet P-40 (Sigma), pH 5.0 for acid sphingomyelinase or pH 7.4 for neutral sphingomyelinase for 5 min on ice. Cells were further disrupted by sonication for 10 min in an ice bath sonicator (Bandelin Electronic, Berlin, Germany). The protein concentration was measured by a Bradford protein assay (BioRad, Feldkirchen, Germany), and 5 μg of protein in 20 μL lysis buffer was added to 250 mM sodium acetate (pH 5.0) containing 100 pmol BODIPY FL C_{12}-sphingomyelin for acid sphingomyelinase or to a buffer of 100 mM HEPES (pH 7.4), 5 mM $MgCl_2$, 0.2% NP40, and 10 μg/mL each of aprotinin and leupeptin containing 100 pmol BODIPY FL C_{12}-sphingomyelin for neutral sphingomyelinase. The samples were incubated at 37 °C for 1 h with shaking at 300 U. The reaction was stopped by the addition of 1 mL chloroform:methanol (2:1, v/v) followed by centrifugation for 5 min at 10,510×*g*. The lower phase was dried in a SpeedVac Concentrator (Thermo Fisher Scientific) and resuspended in 20 μL chloroform:methanol (2:1, v/v). The samples were spotted on a 20-cm thin-layer chromatography (TLC) plate (Merck, Darmstadt, Germany) in 3-μL steps. After all spots were dried, the samples were separated with chloroform:methanol (80:20, v/v), scanned with a Typhoon FLA 9500 laser scanner (GE Healthcare Life Sciences, Freiburg, Germany), and analyzed with Image Quant software (GE Healthcare Life Sciences).

2.5. Sphingolipid quantification by liquid chromatography tandem-mass spectrometry (LC-MS/MS)

Liver tissue homogenates were subjected to lipid extraction using 1.5 mL methanol/chloroform (2:1, v/v) as described before [52]. The extraction solvent contained d_7-sphingosine (d_7-Sph), d_7-sphingosine 1-phosphate (d_7-S1P), C17 ceramide (C17 Cer) and d_{31}-C16 sphingomyelin (d_{31}-C16 SM) (all Avanti Polar Lipids, Alabaster, USA) as internal standards. Chromatographic separations were achieved on a 1260 Infinity II HPLC (Agilent Technologies, Waldbronn, Germany) equipped with a Poroshell 120 EC-C8 column (3.0 × 150 mm, 2.7 μm; Agilent Technologies). MS/MS analyses were carried out using a 6490 triple-quadrupole mass spectrometer (Agilent Technologies) operating in the positive electrospray ionization mode (ESI+). Sph, S1P, Cer and SM were quantified by multiple reaction monitoring (qualifier product ions in parentheses): *m/z* 300.3 → 282.3 (252.3) for Sph, *m/z* 380.3 → 264.3 (82.1) for S1P, $[M\text{-}H_2O + H]^+ \rightarrow m/z$ 264.3 (282.3) for all Cer and $[M+H]^+ \rightarrow m/z$ 184.1 (86.1) for all SM subspecies (C16, C18, C20, C22, C24 and C24:1) [53]. Peak areas of Cer and SM subspecies, as determined with MassHunter Quantitative Analysis software (version 10.1, Agilent Technologies), were normalized to those of the internal standards (C17 Cer or d_{31}-C16 SM) followed by external calibration in the range of 1 fmol–50 pmol on column. Sph and S1P were directly quantified via their deuterated internal standards d_7-Sph (0.25 pmol on column) and d_7-S1P (0.125 pmol on column). Determined sphingolipid amounts were normalized to the actual protein content (as determined by Bradford assay) of the tissue homogenate used for extraction.

2.6. Western blotting

Bone marrow-derived macrophages (BMDMs) were left uninfected or were infected for the indicated times, washed in cold H/S-buffer and lysed for 5–10 min on ice in a lysis buffer, consisting of 25 mM HEPES buffer (125 mM NaCl, 0.1% SDS, 0.5% deoxycholate, 1% Triton, 10 mM EDTA, 10 mM sodium pyrophosphate and 10 mM NaF supplemented with 10 μg/mL Aprotinin/Leupeptin (A/L) and removed from plates with a cell scraper. For in vivo assays, about 5 mg tissue samples were added to 500 μL of the lysis buffer and homogenized with Tissue Lyser (Qiagen) in an Eppendorf tube. Tissue lysates and cell lysates were centrifuged for 10 min at 10,510×*g* at 4 °C. The supernatants were collected, added to 5 × sodium dodecyl sulfate (SDS) sample buffer, and boiled for 5 min at 95 °C. Proteins were separated by 8.5%–12.5% sodium dodecyl sulfate polyacrylamide gel electrophoresis (SDS-PAGE). Samples were blotted on nitrocellulose membranes (Amersham Protran Premium 0.2 μm, product code 10600005; GE Healthcare, Freiburg, Germany) with 80 V at 4 °C for 2 h. Blots were washed with phosphate-buffered saline (PBS) and blocked for 1 h at room temperature in Block Tris-buffered saline (TBS) buffer (Thermo Scientific, Grand Island, NY, USA; supplier number 37542). After another washing step in TBS/Tween (Tris-buffered saline supplemented with 0.1% Tween 20, the membranes were incubated with specific primary antibodies against LC3B (Sigma Aldrich L7543, rabbit IgG), Beclin-1 (BECN1 [H-300], Santa Cruz Biotechnology, Dallas, TX, USA; catalog number, sc-11427), phospho-Akt (Ser 473) (193H12) (Cell Signaling 4058, rabbit IgG), phospho-mTOR (Ser 2448) (D9C2) (Cell Signaling 5536, rabbit IgG), phospho-p38 MAPK (Thr180/Tyr182) (Cell Signaling 9211, rabbit polyclonal), phospho-SAPK/JNK (Thr183/Tyr185) (Cell Signaling 9251, rabbit polyclonal), Cathepsin D (C-20) (Santa Cruz sc-6486, goat polyclonal), Bax (Cell Signaling 2772, rabbit polyclonal), P62/SQSTM1 (Sigma P0067, rabbit polyclonal), cleaved Caspase-3 (Asp 175) (Cell Signaling 9661, rabbit polyclonal) and Caspase-9 (Abcam ab25758, rabbit IgG) overnight at 4 °C in TBS/Tween supplemented with 10% Blocking Buffer. After six washing steps in TBS/Tween, blots were incubated for 1 h at room temperature in TBS/Tween supplemented with 25% Blocking Buffer with alkaline phosphatase (AP)-conjugated secondary antibodies (Santa Cruz Biotechnology). Samples were washed extensively and developed with CDP Star (PerkinElmer, product number NEL616001KT). For normalization of proteins, detection of actin was performed after six washing steps in TBS/Tween as above and incubation for 20 min with anti β-actin antibodies conjugated with HRP (anti-β-actin (C4) HRP; Santa Cruz, sc-47778, mouse IgG). After another 6 washing steps blots were developed with ECL Select Western Blotting Detection Reagent (Amersham, RPN2235).

2.7. TUNEL-assay

Bone marrow-derived macrophages were grown on coverslips, infected or left uninfected. They were then fixed in 4% paraformaldehyde (PFA; Sigma-Aldrich), buffered in PBS consisting of 137 mM NaCl, 2.7 mM KCl, 7 mM $CaCl_2$, 0.8 mM $MgSO_4$, 1.4 mM KH_2PO_4, and 6.5 mM Na_2HPO_4 (pH 7.2–7.4) for 30 min at 4 °C, washed in PBS and permeabilized with 0.2% Triton X-100/PBS for 30 min at room temperature. After a washing step in PBS, the TUNEL reaction was performed exactly as instructed by the vendor (ABP Biosciences, #A051) using Biotin-11-dUTP and Streptavidin conjugated Andy Flour ™594 red fluorescent dye. Samples were counterstained with acid Mayer's Hämalaun (Roth, #T865.1) for 20 s to stain nuclei and washed six times with tap water to bluing for a total of 20 min. Samples were mounted on glass microscope slides with antifading Mowiol (Kuraray Specialities Europe GmbH, Frankfurt, Germany). For positive controls, non-infected cells were incubated with DNase I (2 U/μL) for 30 min at room temperature before the TUNEL reaction. Samples were imaged by Leica DMIRE2 microscope with a 100 × objective lens and apoptotic cells were analyzed by counting at least 100 visual fields/sample. Representative picture was taken with a Keyence, BZ-X810×microscope, 100 × objective lens, Software: Keyence, BZ-X810 Analyzer 1.1.2.4.

2.8. β1-integrin immunoprecipitation

To demonstrate activation of β1-integrin on the surface of bone marrow-derived macrophages (BMDMs), we infected cells for various time periods, removed the medium, and incubated macrophages on ice for 30 min with 1 μg of anti-β1-integrin antibodies, clone 9EG7 (BD), which detects the active conformation of β1-integrin. The samples were washed extensively and lysed in 125 mM NaCl, 25 mM Tris HCl (pH 7.4), 10 mM EDTA, 10 mM sodium pyrophosphate, 3% Nonidet P-40, and 10 μg/mL A/L for 5 min at 4 °C. They were then centrifuged at 10,510×*g*. The immunocomplexes were immobilized with protein A/G agarose (Santa Cruz Biotechnology, Heidelberg, Germany, sc-2003) for 45 min, washed 6 times in lysis buffer, resuspended in 1xSDS Laemmli Sample buffer, and boiled for 5 min at 95 °C. Proteins were separated on 8.5% SDS-PAGE gels, blotted with β1-integrin antibody clone MB1.2 (Merck Chemicals GmbH, Darmstadt, Germany, MAB1997) and developed with an AP-coupled secondary antibody and a chemoluminescence system (Thermo Fisher Scientific).

2.9. Immunohistochemisty

Mice were sacrificed, and tissues were extracted, embedded in Tissue-Tec (Sakura Finetek USA, Torrance, CA, USA), and rapidly frozen in liquid nitrogen. Subsequently, 6 μm thick sections were carefully sliced using a cryotome (CM1850 UV, Leica Microsystems). For the staining procedure, the sections were thawed, allowed to air-dry for 5 min, and then fixed in ice-cold acetone for 10 min. Following this fixation, the samples were washed with PBS and then subjected to blocking for 30 min at room temperature using a solution comprising PBS, 0.05% Tween 20 (Sigma), and 5% fetal calf serum (FCS). The samples were then incubated with monoclonal mouse anti-ceramide antibody (clone S58-9, #MAB0011, Glycobiotech) at a dilution of 1:100 in H/S buffer (containing 132 mM NaCl, 20 mM HEPES [pH 7.4], 5 mM KCl, 1 mM $CaCl_2$, 0.7 mM $MgCl_2$, and 0.8 mM $MgSO_4$) supplemented with 1% FCS at room temperature for 45 min. Following the primary antibody incubation, the samples underwent three washes with PBS containing 0.05% Tween 20 and an additional wash with PBS. The tissue sections were subsequently subjected to secondary labeling for 30 min using Cy3-coupled anti-rat/rabbit/mouse F $(ab)_2$ fragments (Jackson Immunoresearch) in H/S buffer supplemented with 1% FCS. Post-labeling, the samples were washed three times with PBS containing 0.05% Tween 20, followed by a final wash with PBS. Finally, the stained tissue sections were embedded in Mowiol. The samples were then evaluated by confocal microscopy. Images were quantified with ImageJ.

2.10. Determination of cytokines

Blood samples were collected from mice and then centrifuged at 1000×*g* for 10 min at 4 °C to separate the plasma. The levels of cytokines were determined using the LEGENDplex mouse inflammation panel (BioLegend, #740446), following the manufacturer's instructions. The analysis was carried out on an Attune NxT machine, and the LEGENDplex data analysis software provided by BioLegend was used for data analysis.

2.11. Statistical analysis

All data were obtained from at least 3 independent experiments and expressed as arithmetic mean ± standard deviation (SD). We tested all results for normal distribution using the David Pearson-Stephens test. Statistical analysis was performed using Student's t-test for single comparisons or with analysis of variance (ANOVA) for multiple comparisons. GraphPad Prism 9 statistical software (GraphPad Software, La Jolla, CA, USA) was used for the analysis. P-values <0.05 were regarded as statistically significant.

3. Results

3.1. Caveolin-1 deficiency leads to reduced killing of BCG by macrophages and to higher bacterial burden during acute phase of infection in mice

To elucidate the relevance of Caveolin-1 in mycobacterial infection, we intravenously injected Wt or Caveolin-1 deficient mice ($Cav1^{-/-}$) with 1×10^7 bacteria to obtain a systemic infection and determined bacterial numbers by colony forming unit (CFU) assays in tissues after 1 week (acute phase) or 3 weeks (advanced phase) of infection. We focused on the analysis of livers, because, in comparison to splenic macrophages/peritoneal macrophages, liver macrophages (Kupffer cells) have been shown to play a critical role in mycobacterial infections [54]. We found an approximately 30% lower hepatic burden of BCG in Wt mice compared to Caveolin-1 deficient mice ($Cav1^{-/-}$) after 1 week of infection (Fig. 1A), but no significant difference after 3 weeks of infection (Fig. 1B). To validate bacterial killing in vitro, we infected bone marrow-derived macrophages with BCG for 6 h with a bacteria-to-host cell ratio (multiplicity of infection, MOI) of 50:1. Bone marrow-derived macrophages have been reported to have similar biological functions as Kupffer cells [55]. The colony forming unit (CFU) assays revealed that cells from Caveolin-1 ($Cav1^{-/-}$) deficient mice contained about 20% more bacteria than macrophages from Wt mice (Fig. 1C). This suggests that the absence of Caveolin-1 leads to reduced killing of BCG by macrophages and a reduced control of the mycobacteria during acute phase of infection *in vivo*.

3.2. Caveolin-1 deficiency does not affect internalization or activation of neutral sphingomyelinase after BCG infection in vivo and in vitro

To clarify the mechanisms, how Caveolin-1 deficiency leads to increased susceptibility during early infection, we tested whether the internalization upon BCG infection was altered in Caveolin-1 deficient macrophages. To this end, we infected bone marrow-derived macrophages with BCG for 5 or 30 min with a bacteria-to-host cell ratio (multiplicity of infection, MOI) of 10:1 and determined bacterial uptake by performing colony-forming unit (CFU) assays. As shown in Fig. 2A, no difference in BCG internalization between Wt and Caveolin-1 deficient ($Cav1^{-/-}$) cells was observed (Fig. 2A).

We have previously shown that BCG infection is promoted by the expression of neutral sphingomyelinase-2 (Nsm2), which regulates a signaling cascade via the p38-mitogen-activated protein kinase (p38 K) and c-Jun N-terminal kinases (pSAPK/JNK), leading to the activation of surface β1-integrin and triggering granuloma formation, which is crucial

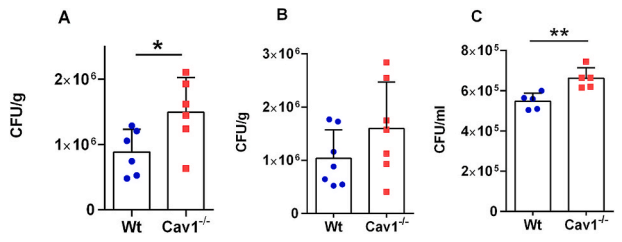

Fig. 1. Caveolin-1 deficiency leads to reduced killing of BCG by macrophages and to higher bacterial burden during acute phase of infection in mice. (**A-B**) Wt or Caveolin-1 deficient (Cav1$^{-/-}$) mice were intravenously infected with 1 × 10^7 BCG for 1 week (**A**) or 3 weeks (**B**), mice were sacrificed, livers were removed and colony-forming units (CFU) were determined after 2 weeks of culture. (**C**) Bone marrow-derived macrophages obtained from Wt or Caveolin-1 deficient (Cav1$^{-/-}$) mice were infected with BCG for 6 h with a bacteria-to-host cell ratio (multiplicity of infection, MOI) of 50:1, cells were lysed with saponin and colony-forming units (CFU) were determined (**C**). Shown are the means ± standard deviation (SD) of the numbers of bacteria, n = 4–6, *t*-test, *p = 0.039 (**A**), **p = 0.0047 (**C**).

for mycobacterial infection *in vitro* and *in vivo* [56]. We therefore determined the activity of neutral sphingomyelinase-2 (Nsm2), the activation of surface β1-integrin and the phosphorylation of p38 K and JNK in Wt and Caveolin-1 deficient (Cav1$^{-/-}$) macrophages upon BCG infection at various time points after infection with a bacteria-to-host cell ratio (multiplicity of infection, MOI) of 10:1 and compared them with non-infected cells. The results show a slight, but not significant increase of the neutral sphingomyelinase-2 (Nsm2) activity and of active β1-integrin on the surface of the cells after 1–5 min (summarized) infection with BCG (Fig. 2B and C), but no difference between Wt and Caveolin-1 deficient (Cav1$^{-/-}$) bone marrow-derived macrophages (Fig. 2B and C). We then determined mitogen-activated protein kinase (MAPK) cascades, which are key signaling pathways that regulate a wide variety of cellular processes [57]. To this end, we detected p38-kinase (p38 K) and c-Jun-N-terminal kinase (pSAPK/JNK) by Western blotting at various time points after infection with a bacteria-to-host cell ratio (multiplicity of infection, MOI) of 10:1 and compared them with non-infected cells. The results showed marked phosphorylation of p38 K after 5 min of infection, which persisted until 90 min of infection, but phosphorylation was similar in Wt and Caveolin-1 deficient (Cav1$^{-/-}$) cells after BCG infection (Fig. 2D). Likewise, the results from Western blot studies of SAPK/JNK also demonstrated a strong increase upon BCG infection after 5 and 30 min of infection compared to non-infected cells, in both Wt and Caveolin-1 deficient (Cav1$^{-/-}$) macrophages without difference (Fig. 2E).

3.3. Autophagy is not critical for BCG infection in Caveolin-1 deficient mice and macrophages

We and others have previously demonstrated that autophagy serves as an important host immune defense mechanism during infection with *Mycobacterium tuberculosis* and BCG and functions as a key regulator of inflammation [58–61]. Therefore, autophagy-associated proteins were investigated *in vivo* and *in vitro*. For *in vitro* examination, we infected bone marrow-derived macrophages from Wt and Caveolin-1 deficient (Cav1$^{-/-}$) mice for the indicated times with BCG or left them uninfected, and performed Western blotting for the autophagy-associated proteins phosphorylated mammalian target of rapamycin (pmTOR), phosphorylated AKT (pAKT), microtubule-associated protein 1 light chain 3 beta (LC3B), p62 and cathepsin D (CTSD). Results revealed that the levels of phospho-mTOR did not significantly change upon infection with BCG, neither in Wt, nor in Caveolin-1 deficient (Cav1$^{-/-}$) macrophages (Fig. 3A). Phosphorylation of AKT was significantly upregulated after 30 min of infection with BCG, similar in both genotypes (Fig. 3B). The analysis of LC3B, p62 and CTSD in bone marrow-derived macrophages revealed no significant changes upon infection with BCG (Fig. 3C–E).

In vivo, we again focused on liver and determined the levels of LC3B, phosphorylated Beclin (pBeclin), p62 and cathepsin D (CTSD) in Wt and Caveolin-1 deficient (Cav1$^{-/-}$) mice after systemic infection with BCG for 1 or 3 weeks. The results reveal that LC3B was significantly increased in Caveolin-1 deficient (Cav1$^{-/-}$) and Wt livers 3 weeks after infection compared to non-infected controls, but not after 1 week of infection (Fig. 3F–S1). The increase of LC3B expression was more pronounced in Caveolin-1 deficient (Cav1$^{-/-}$) livers than in Wt mice (Fig. 3F–S1). In contrast, we did not detect differences in the expression of pBeclin (Fig. 3G–S2), p62 (Fig. 3H–S3) and CTSD (Fig. 3I–S4) between non-infected and infected samples, as well as between both genotypes.

3.4. Caveolin-1 regulates cell death upon BCG infection

Caveolin-1 has been linked to cell death signaling pathways and apoptosis [23–27]. It has been described that BCG infection of murine macrophages effectively induces apoptosis by stimulation of Caspase 3, 9 and 12, thereby controlling intracellular bacteria [62]. To elucidate, if interference of apoptosis is responsible for higher susceptibility of Caveolin-1 deficient mice to early BCG infection, we first determined the number of apoptotic cells in infected bone marrow-derived macrophages Wt and Caveolin-1 deficient (Cav1$^{-/-}$) cells upon BCG infection for 6 or 24 h with a bacteria-to-host cell ratio (multiplicity of infection, MOI) of 50:1 via TUNEL-assay. The results revealed that the number of apoptotic cells increased with time in both, Wt and Caveolin-1 deficient (Cav1$^{-/-}$) cells (Fig. 4A). However, much more apoptotic cells were detected after 24 h in Caveolin-1 deficient macrophages compared to Wt cells. Uninfected cells of both genotypes showed no notable apoptosis (Fig. 4A). To follow up the evidence for increased cell death in Caveolin-1 deficient mice upon mycobacterial infection, we detected the expression of different markers, which are important in apoptotic processes *in vitro* and *in vivo*. To this end, we infected bone marrow-derived macrophages from Wt and Caveolin-1 deficient (Cav1$^{-/-}$) mice with BCG for the indicated time, lysed the cells and performed Western blotting for cleaved Caspase 3, Caspase 9 and Bax proteins. The results revealed that Caspase 9, which is involved in key step in the intrinsic pathway of apoptosis [63], was significantly upregulated upon infection with BCG over time, with a maximum at 5 min of infection only in Caveolin-1 deficient (Cav1$^{-/-}$), but not in Wt cells (Fig. 4B). Western blot analysis of Bax revealed, that Bax expression moderately increased in Caveolin-1 deficient (Cav1$^{-/-}$) macrophages, which was significantly different from Wt macrophages since these show no differences at all (Fig. 4C). The expression of cleaved Caspase 3 was neither different between both genotypes, nor upregulated upon infection with BCG in both genotypes (Fig. 4D).

For *in vivo* detection of apoptotic markers, we infected Wt or Caveolin-1 deficient (Cav1$^{-/-}$) mice intravenously with 1 × 10^7 BCG for 1 and 3 weeks or left them uninfected, sacrificed them, removed tissues and performed Western blots from mouse liver lysates for Bax, cleaved Caspase 3 and Caspase 9. The results revealed that Caveolin-1 deficient (Cav1$^{-/-}$) mice showed a remarkable upregulation of Bax expression in the livers upon infection with BCG for 1 week, which normalized within 3 weeks (Fig. 4E–S5). In contrast, Wt livers did not show any increase of Bax during infection, neither after 1 nor after 3 weeks of infection (Fig. 4E, S5). We did not measure any notable expression of cleaved Caspase 3 in uninfected livers, and as observed in macrophages, the expression of cleaved Caspase 3 also did not change upon infection in Caveolin-1 deficient (Cav1$^{-/-}$) and Wt mice (Fig. 4F–S6). Instead, Caspase 9 expression increased in Caveolin-1 deficient (Cav1$^{-/-}$) mice after 1 week of infection, compared to non-infected controls or Wt tissues, and then normalized after 3 weeks of infection to the level of uninfected controls (Fig. 4G–S7). In summary, these examinations indicate that, compared to Wt mice, cell death pathways are enhanced in Caveolin-1 deficient mice upon mycobacterial infection.

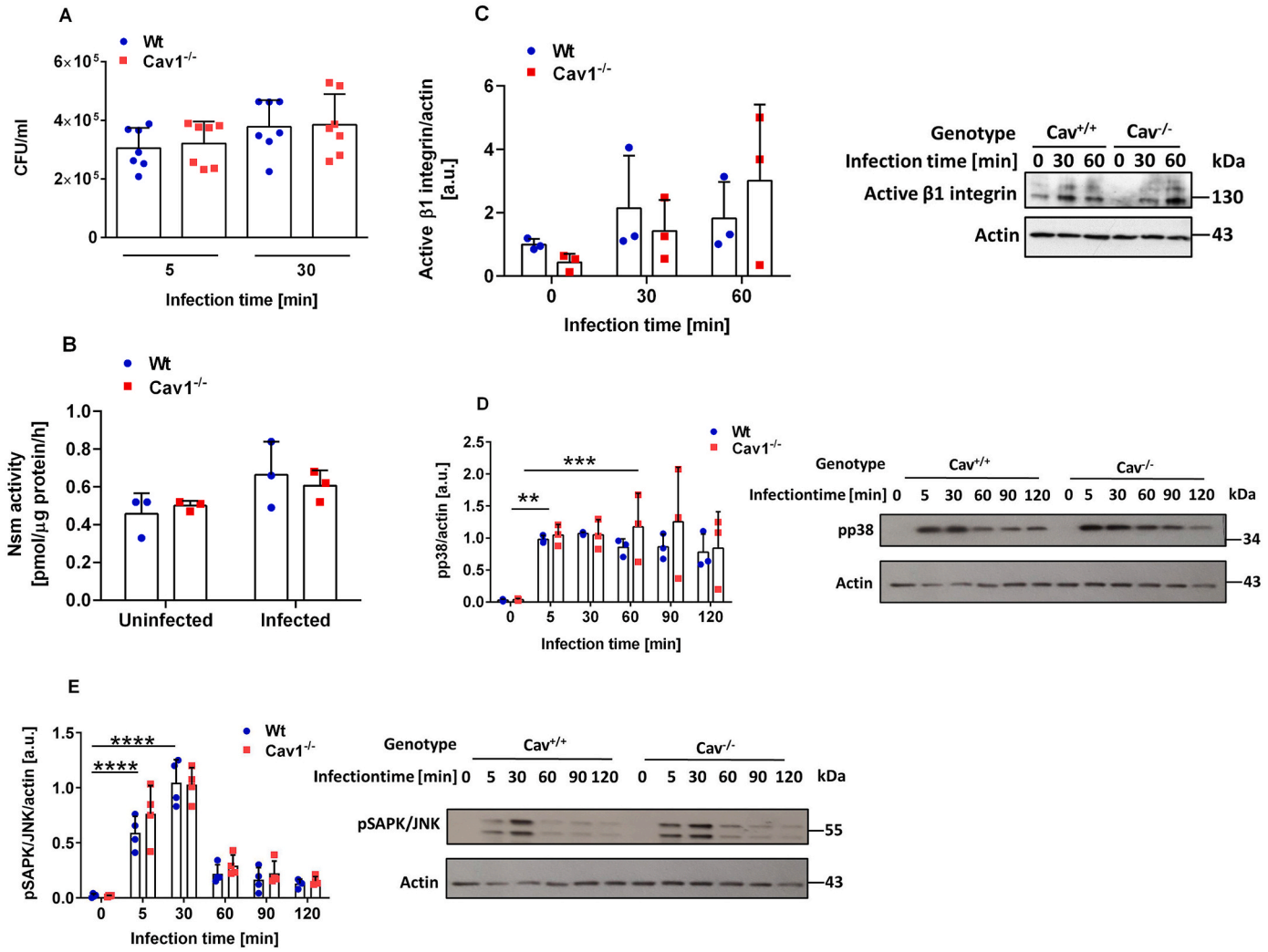

Fig. 2. Caveolin-1-deficiency does not affect internalization or activation of neutral sphingomyelinase after BCG infection *in vivo* and *in vitro* (**A**) Bone marrow-derived macrophages from Wt or Caveolin-1 deficient ($Cav1^{-/-}$) mice were infected with BCG for the indicated times with a with a bacteria-to-host cell ratio (multiplicity of infection, MOI) of 10:1 and colony-forming unit (CFU) assay was performed. (**B**) Macrophages from Wt or Caveolin-1 deficient ($Cav1^{-/-}$) mice were infected with BCG for 1–5 min (summarized) or left uninfected and of neutral sphingomyelinase 2 (Nsm2) activity was determined. Shown are means ± SD, n = 7 (**A**), n = 3 (**B**), ANOVA, followed by Bonferroni's multiple comparisons test. (**C**) Active β1-integrin expression of macrophages from Wt or Caveolin-1 deficient ($Cav1^{-/-}$) mice was determined in uninfected cells or after BCG infection (MOI 10:1) for 30 or 60 min by immunoprecipitation. Shown is the quantitative analysis of Westernblots (n = 3) as determined by ImageJ and presented in arbitrary units (a.u.), ANOVA, followed by Bonferroni's multiple comparisons test and a representative blot. (**D-E**) Wt or Caveolin-1 deficient ($Cav1^{-/-}$) bone marrow-derived macrophages were infected with BCG (MOI 10:1) for the indicated times or left uninfected. Cells were lysed and Western blots were performed for pp38 (**D**) or pSAPK/JNK (**E**) as described. Shown are the means ± SD of the quantitative analyses of the blots from 3 to 4 experiments, p-values were calculated by ANOVA followed by Bonferroni's multiple comparisons test (**D-E**), *p < 0.1, **p < 0.01, ***p < 0.001, ****p < 0.0001, and representative blots.

3.5. Acid sphingomyelinase-derived ceramide is increased in Caveolin-1 deficient mice upon BCG infection

A variety of studies demonstrated a central role for the acid sphingomyelinase (Asm) and ceramide in several forms of cell death [64–67]. Ceramide seems to induce and regulate the activity of certain proteins, which act as apoptosis regulators in several cell types, including macrophages [68,69]. To find out, if Caveolin-1 expression regulates acid sphingomyelinase (Asm) prior and/or upon infection, we determined the activity of acid sphingomyelinase (Asm) in non-infected bone marrow-derived macrophages from Wt and Caveolin-1 deficient ($Cav1^{-/-}$) mice and after infection with BCG for the indicated time points (Fig. 5A). The results showed, that acid sphingomyelinase activity was generally higher in Caveolin-1 deficient ($Cav1^{-/-}$) macrophages than in syngenic Wt cells, also before infection, and increased similarly in both, Wt and Caveolin-1 deficient ($Cav1^{-/-}$) macrophages, after infection with a maximum of 30 min (Fig. 5A).

The acid sphingomyelinase (Asm) hydrolyzes sphingomyelin to form ceramide [reviewed in 70 and 71], which continues to be metabolized into bioactive sphingolipids, such as sphingosine, respectively sphingosine 1-phosphate [reviewed in 72]. To follow the indication of increased acid sphingomyelinase activity in Caveolin-1 deficient ($Cav1^{-/-}$) macrophages, we infected Wt and Caveolin-1 deficient ($Cav1^{-/-}$) mice systemically with BCG for 1 and 3 weeks or let them uninfected, sacrificed the mice, removed livers and determined ceramide, sphingomyelin (SM), sphingosine (Sph) and sphingosine 1-phosphate (S1P) by LC-MS/MS (Fig. 5B–E). The results reveal that livers from Caveolin-1 deficient ($Cav1^{-/-}$) mice exhibited a strong increase of ceramide after 3 weeks, but not after 1 week of infection with BCG compared to non-infected controls (Fig. 5B). This was in contrast to Wt livers, which did not show a significant increase of ceramide upon BCG infection, although we observed a trend of an increase of ceramide in Wt livers 3 weeks after infection (Fig. 5B). Measurement of sphingomyelin (SM) demonstrated, that livers from Wt mice exhibited a slight increase

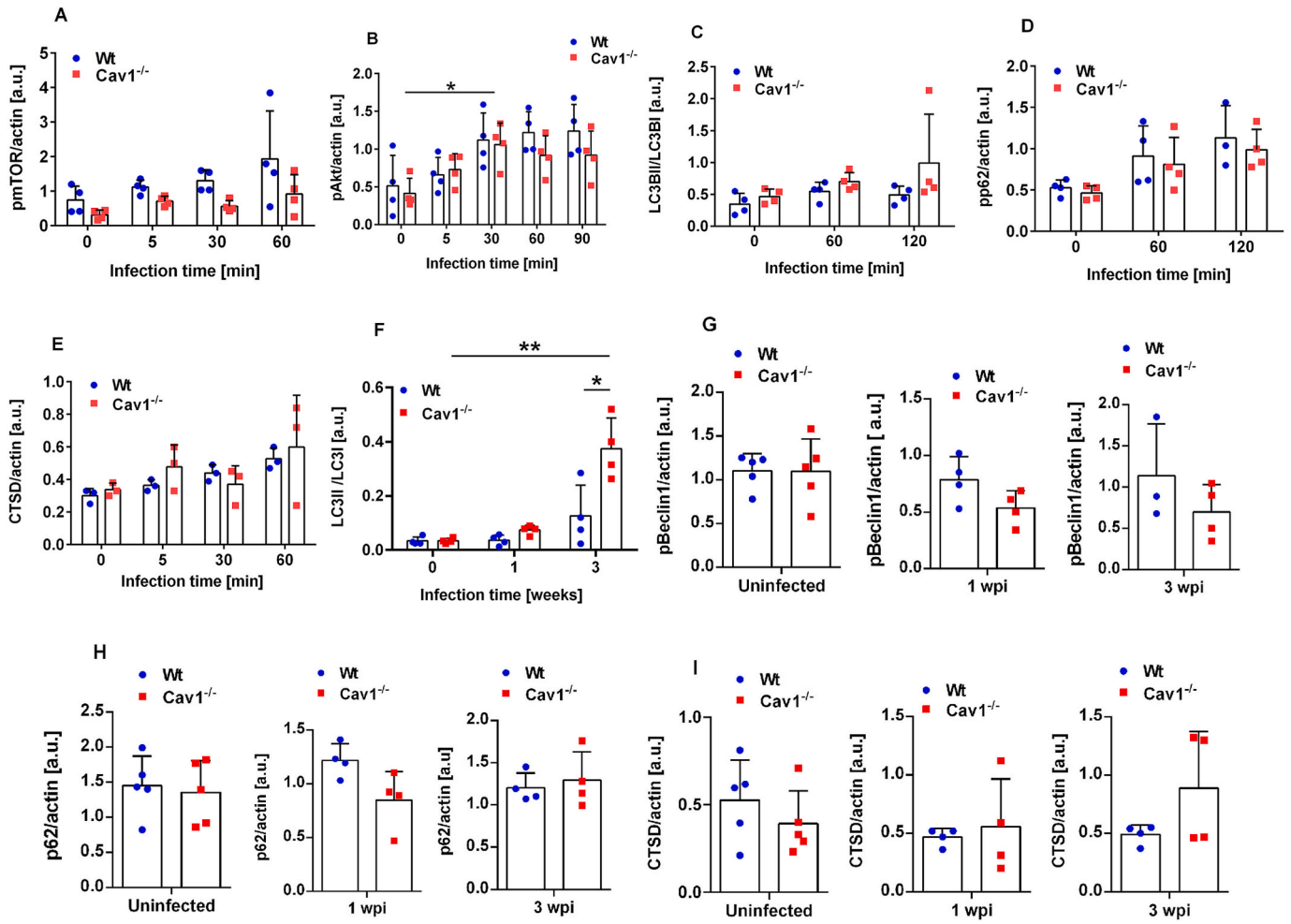

Fig. 3. Autophagy is not critical for BCG infection in Caveolin-1 deficient mice and macrophages (**A-E**) Bone marrow-derived macrophages from Wt or Caveolin-1 deficient ($Cav1^{-/-}$) mice were infected with BCG for the indicated times with a with a bacteria-to-host cell ratio (multiplicity of infection, MOI) of 10:1 or left uninfected. Cells were lysed and Western blots were performed for pmTOR (**A**), pAKT (**B**), LC3B (**C**), p62 (**D**) or CTSD (**E**) as described. Shown are the means ± SD of the quantitative analysis of the blots from 3 to 4 experiments, p-values were calculated by ANOVA followed by Bonferroni's multiple comparisons test (**A-E**), *p < 0.1. (**F–I**) Wt or Caveolin-1 deficient ($Cav1^{-/-}$) mice were systemically infected with 1×10^7 BCG for 1 or 3 weeks or left uninfected, mice were sacrificed, livers were removed, lysed and Westernblots for LC3B (**F**), pBeclin (**G**), p62 (**H**) and CTSD (**I**) were performed. Expression of proteins was normalized to actin levels and quantification of the densities given as arbitrary units (a.u.) was performed using ImageJ. Displayed are the means ± SD of 3–4 experiments, p-values were calculated by ANOVA followed by Bonferroni's multiple comparisons test (**F–I**), *p < 0.01, **p < 0.01.

in the level of sphingomyelin (SM) after 3 weeks of infection with BCG, whereas Caveolin-1 deficient ($Cav1^{-/-}$) mice did not show any changes (Fig. 5C). The level of sphingosine (Sph) and sphingosine 1-phosphate (S1P) did not differ between infected and uninfected livers, or between both genotypes (Fig. 5D and E). To summarize the consumption of sphingomyelin (SM) to ceramide upon infection with BCG, the sphingomyelin (SM)/ceramide (Cer) ratio was calculated. This analysis demonstrates that Caveolin-1 deficient ($Cav1^{-/-}$) livers exhibited a strong reduction of sphingomyelin (SM)/ceramide (Cer) ratio compared to non-infected controls 3 weeks after BCG infection (Fig. 5F), while the sphingomyelin (SM)/ceramide (Cer) ratio in livers of Wt mice did not show significant changes upon infection (Fig. 5F). Ceramide stainings in livers confirmed the data measured by LC-MS/MS. In comparison to uninfected controls or Wt tissues, Caveolin-1 deficient ($Cav1^{-/-}$) livers exhibited a significant increase of ceramide already after 1 week of infection with BCG, which was even more evident upon 3 weeks of infection (Fig. 5G). These results indicate that Caveolin-1 regulates acid sphingomyelinase (Asm)-induced ceramide formation upon mycobacterial infection.

3.6. *Inflammatory cytokines are dysregulated in Caveolin-1 deficient mice upon BCG infection*

Inflammatory cytokines play a major role in host defense against *Mycobacterium tuberculosis* or other mycobacteria. Particularly interferon γ (IFNγ) and tumor necrosis factor α (TNFα) are essential for survival following *Mycobacterium tuberculosis* infection, by coordinating and maintaining mononuclear inflammation, induction of innate cytokine and chemokine responses and phagocyte activation [73,74]. To investigate if Caveolin-1 regulates the production of inflammatory cytokines during BCG infection in mice, we infected Wt and Caveolin-1 deficient ($Cav1^{-/-}$) mice systemically with BCG for 1 and 3 weeks or left them uninfected, obtained blood serum and determined the concentrations of different cytokines. The results reveal an increase of interferon γ (IFNγ) (Fig. 6A) and tumor necrosis factor α (TNFα) (Fig. 6B) after 3, but not after 1 week of infection in both genotypes compared to non-infected controls (6 A-B). Of note, compared to Wt mice, Caveolin-1 deficient ($Cav1^{-/-}$) mice exhibited a remarkable weaker increase of IFNγ (Fig. 6A) and TNFα (Fig. 6B) 3 weeks after infection. Determination of interleukin-6 (IL-6) showed that compared to non-infected controls Wt mice exhibited a strong increase of interleukin-6 (IL-6) upon

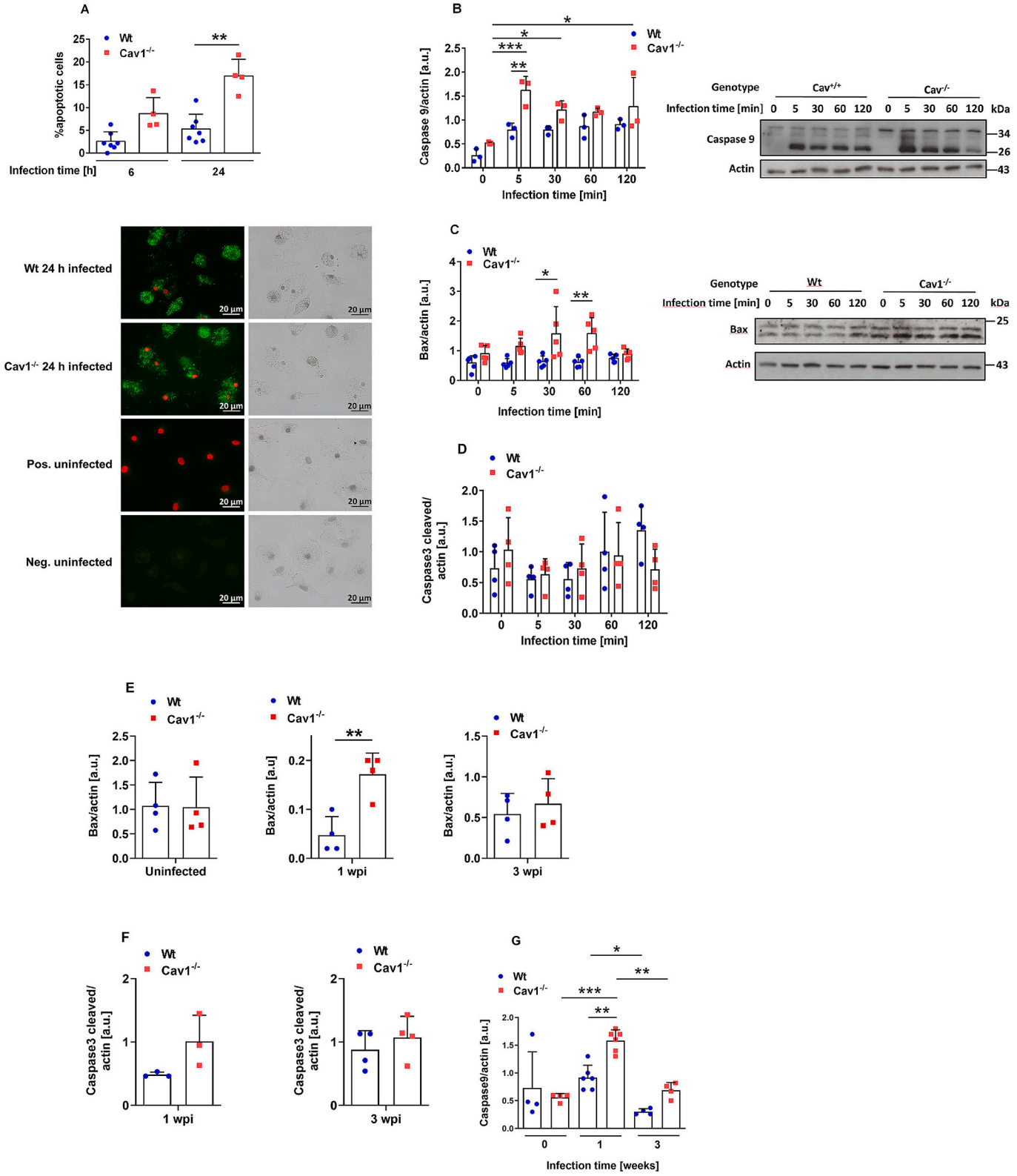

Fig. 4. Caveolin-1 regulates cell death upon BCG infection (**A**) Bone marrow-derived macrophages derived from Wt and Caveolin-1 deficient (Cav1$^{-/-}$) mice were infected with BCG for 6 or 24 h with a with a bacteria-to-host cell ratio (multiplicity of infection, MOI) of 50:1 and the number of apoptotic cells was determined via TUNEL-assay. Shown are the means ± standard deviation (SD) (n = 4–7), ANOVA, followed by Bonferroni's multiple comparison test, **p = 0.0061 and a representative picture, scale bar is 20 µm. (**B-D**) Bone marrow-derived macrophages from Wt and Caveolin-1 deficient (Cav1$^{-/-}$) mice were infected with BCG (MOI 10:1) for the indicated times or left uninfected, lysed and Westernblots on Caspase 9 (**B**), Bax (**C**) or cleaved Caspase 3 (**D**) were performed. (**E-G**) Wt and Caveolin-1 deficient (Cav1$^{-/-}$) mice were intravenously infected with 1×10^7 BCG for 1 or 3 weeks, sacrificed, livers were removed and lysed. The apoptotic markers Bax (**E**), cleaved Caspase 3 (**F**) and Caspase 9 (**G**) were detected via Western blotting. Shown is the quantitative analysis of Westernblots (n = 3–6) as determined by ImageJ and presented in arbitrary units (a.u.), ANOVA, followed by Bonferroni's multiple comparisons test (**B-G**) and representative blots (**B**, **C**), *p < 0.1, **p < 0.01, ***p < 0.001.

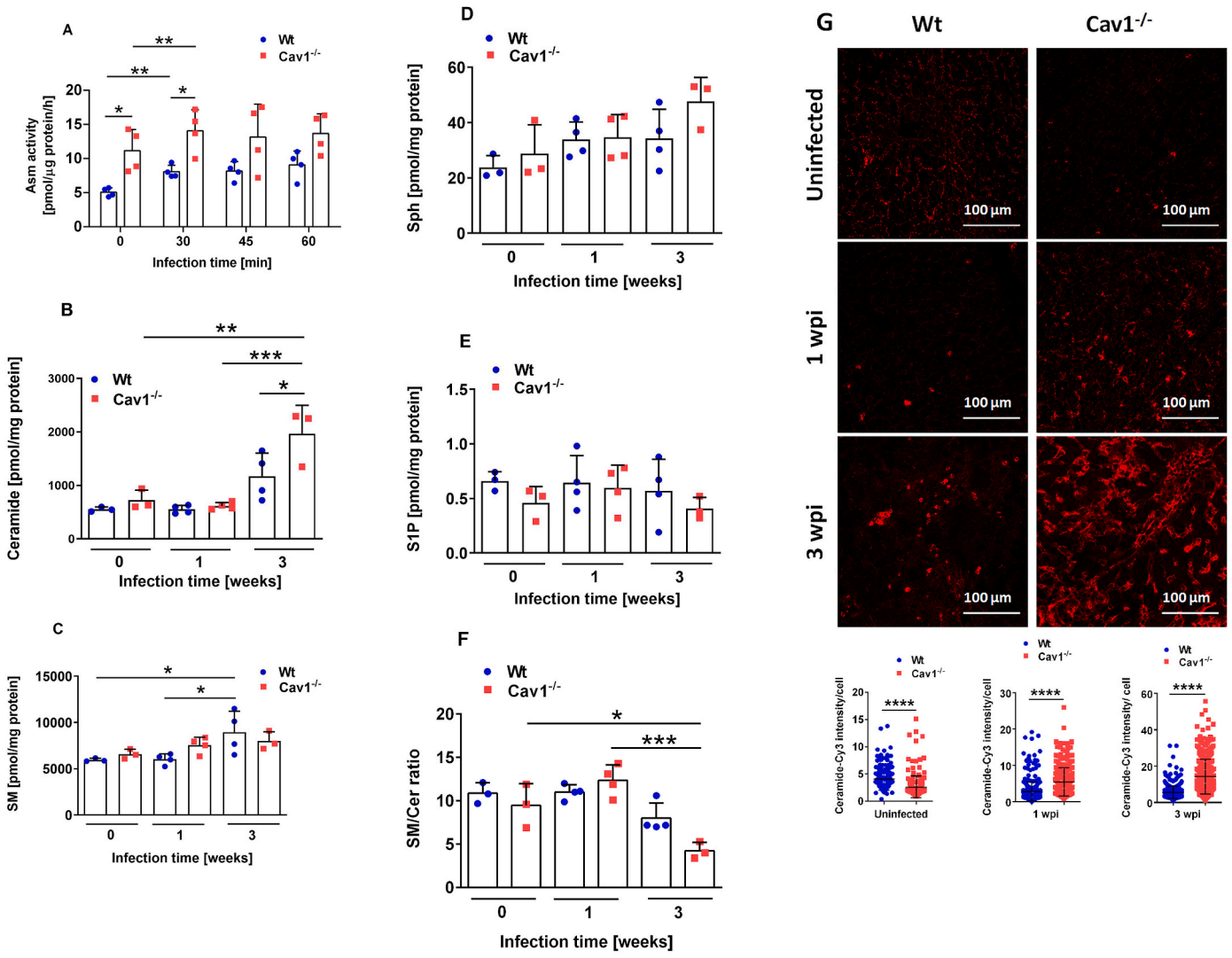

Fig. 5. Acid sphingomyelinase-derived ceramide is increased in Caveolin-1 deficient mice upon BCG infection (**A**) Bone marrow-derived macrophages from Wt and Caveolin-1 deficient ($Cav1^{-/-}$) mice were infected with BCG with a bacteria-to-host cell ratio (multiplicity of infection, MOI) of 10:1 for the indicated time, lysed and the activity of acid sphingomyelinase (Asm) was measured with green fluorescent BODIPY FL C_{12}-sphingomyelin. Shown are the means ± SD of the acid sphingomyelinase activity from 4 independent experiments, ANOVA, *p < 0.1, **p < 0.01. (**B–F**) Wt and Caveolin-1 deficient ($Cav1^{-/-}$) mice were systemically infected with 1×10^7 BCG for 1 or 3 weeks or left uninfected, sacrificed, livers were removed, homogenized and subjected to lipid extraction. Ceramide (**B**), sphingomyelin (SM) (**C**), sphingosine (Sph) (**D**) and sphingosine-1-phosphate (S1P) (**E**) were quantified by liquid chromatography tandem-mass spectrometry (LC-MS/MS), normalized to proteins and displayed as pmol/mg protein. The sphingomyelin (SM)/ceramide (Cer) ratio (SM/Cer ratio) was calculated (**F**). Shown are the means ± SD from 3 to 4 independent experiments, p-values were determined by ANOVA followed by Bonferroni's multiple comparisons test, *p < 0.1, **p < 0.01, ***p < 0.001. (**G**) Wt and Caveolin-1 deficient ($Cav1^{-/-}$) mice were systemically infected with 1×10^7 BCG for 1 or 3 weeks or left uninfected, sacrificed, livers were removed and subjected to histopathologic assessment of ceramide. Shown is the quantitative analysis of 3 stainings, ANOVA followed by Bonferroni's multiple comparisons test *p < 0.1, **p < 0.01, ***p < 0.001. Representative pictures are taken with a Leica SP5 confocal microscope, scale bar is 100 µm. (For interpretation of the references to colour in this figure legend, the reader is referred to the Web version of this article.)

infection for 3 weeks, but not for 1 week of infection. This increase of IL-6 was absent in Caveolin-1 deficient ($Cav1^{-/-}$) mice (Fig. 6C). Other cytokines, as Monocyte chemoattractant protein-1 (MCP-1), interleukin-12p70 (IL-12p70), interleukin-1β (IL-1β), interleukin-23 (IL-23), interleukin-1α (IL-1α), interleukin-10 (IL-10), interleukin-27 (IL-27), interleukin-17 A (IL-17 A), interferon β (IFNβ) or granulocyte macrophage-colony stimulating factor (GM-CSF) showed no difference between both genotypes (not shown). These results suggest that Caveolin-1 expression is necessary to adequately induce prominent inflammatory cytokines upon infection of mice with BCG.

4. Discussion

To elucidate the role of Caveolin-1 in mycobacterial infections, we determined a variety of parameters in the course of bacterial infection in Wildtype (Wt) mice compared to Caveolin-1 deficient ($Cav1^{-/-}$) mice and macrophages after infection with *Mycobacterium bovis* Bacillus Calmette-Guérin (BCG), as model for tuberculosis. We show that, compared to Wt mice, the infection of Caveolin-1 deficient mice with BCG leads to moderately higher bacterial burdens in the acute phase of infection in the livers and observed a tendency to more bacteria during the advanced/sub-chronic course of infection. Notably, the absence of Caveolin-1 also results in a reduced early killing of BCG in macrophages. To better understand the circumstances of extrapulmonary or disseminated *M. tuberculosis* infections and to be consistent with previous studies of our group, we chose intravenous instead of intranasal infection, and although information on organs other than the liver would also be of interest, we limited our study to the liver, as it has been shown that

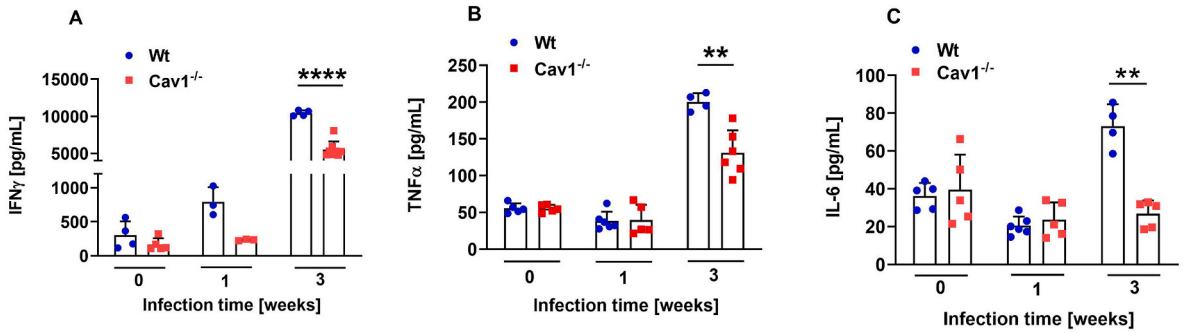

Fig. 6. Inflammatory cytokines are dysregulated in Caveolin-1 deficient mice upon BCG infection (**A-C**) Wt and Caveolin-1 deficient ($Cav1^{-/-}$) mice were intravenously infected with 1×10^7 BCG for 1 or 3 weeks or left uninfected, sacrificed, serum was taken, and interferon γ (β γ) (**A**), tumor necrosis factor α (TNFα) (**B**) and interleukin 6 (IL-6) (**C**) were determined using the LEGENDplex mouse inflammation kit. Displayed are the means ± SD from 3 to 5 experiments, p-values were calculated by ANOVA followed by Bonferroni's multiple comparisons test, $^{**}p < 0.01$, $^{****}p < 0.0001$. Note on INF_Y,1 week: Some values were extremely high/out of range, so we only included values that were within the measurement range of the LEGENDplex inflammation panel in the statistical analysis.

hepatic macrophages (Kupffer cells), in contrast to spleen macrophages/peritoneal macrophages, play a critical role in mycobacterial infections [54].

A typical hallmark of mycobacterial infection is the formation of granulomas, composed mainly of epitheloid macrophages, multinucleated giant cells and foamy macrophages, which are recognized to be host defense mechanisms [75,76]. The constitution of granuloma differs during acute and persistent phases of infection. In the early stage, the formation of granuloma is characterized by the development of inflammatory infiltrates in host tissues, accompanied by a clear predominance of T-helper 1 (Th1) cells [77]. This is followed by a chronic or advanced phase, starting at 3 weeks, manifested by the appearance of matured granuloma and histopathological changes, indicative of more severity and associated with enhanced $CD4^+$ T-cell priming [78]. The transition from the acute to the chronic phase of infection is also associated with a shift in cytokine production. During early mycobacterial infection, high concentrations of interleukin-2 (IL-2), interleukin-1 (IL-1), and tumor necrosis factor α (TNFα), low levels of transforming growth factor β (TGF-β), as well as an incremental increase of interferon γ (IFNγ) have been described, whereas the persistent or chronic infection is characterized by a decrease in interleukin-1 (IL-1), interleukin-2 (IL-2), and tumor necrosis factor α (TNFα), accompanied with very high levels of transforming growth factor β (TGFβ) and interferon γ (IFNγ) [77,79,80]. The measurements of cytokines in our studies also revealed a shift in cytokine production from the early to the advanced course of infection with BCG. We observed an increase of interferon γ (IFNγ), tumor necrosis factor α (TNFα) and interleukin-6 (IL-6) upon infection only after 3 weeks infection, but not after 1 week of infection. This pattern was observed in Wt mice as well as in Caveolin-1 deficient ($Cav1^{-/-}$) mice. However, cytokines increase after 3 weeks of infection was much lower for Caveolin-1 deficient ($Cav1^{-/-}$) mice than for Wt mice. These results indicate a delayed activation of the immune system upon infection with BCG for the prominent cytokines IFNγ, TNFα and IL-6 in our model, in particular in Caveolin-1 deficient mice.

Previous studies demonstrated an increased sensitivity of Caveolin-1 deficient ($Cav1^{-/-}$) mice to *Pseudomonas aeruginosa* [28], *Salmonella enterica* serovar Typhimurium [29], and *Klebsiella pneumonia* [30] infections, as indicated by an increased mortality rate, elevated bacterial burdens recovered from lungs and spleens, and elevated inflammatory responses. In addition, Caveolin-1 deficiency has been shown to impair the infection of murine monocytic myeloid-derived suppressor cells with BCG due to a selective defect of intracellular Toll-like receptor (TLR)2 levels, which leads to reduced capacity to generate various cytokines, to upregulate surface markers and to induce nitrogen oxide (NO) production [40]. Further, in a sepsis model Caveolin-1 deficient ($Cav1^{-/-}$) mice exhibited decreased mortality due to decreased levels of inflammation mediated by interactions with nitric oxide [81]. These studies indicate multi-faceted roles for Caveolin-1 in infectious diseases. Our findings of moderately elevated BCG burden in Caveolin-1 deficient ($Cav1^{-/-}$) mice in the early course of the infection and in macrophages are consistent with the observations for *Pseudomonas aeruginosa*, *Salmonella enterica* serovar Typhimurium and *Klebsiella pneumonia*. However, in our experiments Caveolin-1 deficient ($Cav1^{-/-}$) mice showed less inflammatory responses than Wt mice to BCG. A reasonable explanation might be that in contrast to the mentioned bacteria, mycobacteria have to suppress the immune system to survive and therefore aim to delay the initiation of innate and adaptive immunity to resist immune clearance. Multiple reports previously described that pathogenic mycobacteria inhibit several aspects of the innate and adaptive immune response during infection, including phagosome maturation or cytokine production [82–86]. Thus, it could be, that the impaired defense of Caveolin-1 deficient ($Cav1^{-/-}$) mice and macrophages to BCG, compared to Wt mice, is due to insufficient formation of cytokines required for effective killing. After 3 weeks of infection, numbers of BCG in livers from Wt- and Caveolin-1 deficient mice did not differ anymore, because immune response was increased and, although weaker in Caveolin-1 deficient mice, sufficient enough to eliminate mycobacteria.

The increased bacterial load in livers of Caveolin-1 deficient mice and in macrophages during the early phase of the infection was not due to impaired internalization of BCG by host macrophages (see Fig. 2A), which are the major cell type infected by *Mycobacterium tuberculosis* and BCG [87]. This is consistent with the findings of other groups challenging macrophages from Wt or Caveolin-1 deficient mice with *Salmonella enterica* serovar Typhimurium or murine monocytic suppressor cells with BCG [29,40].

Sphingomyelinases are enzymes characterized by their pH dependency: acid, neutral, and alkaline sphingomyelinases have been identified [88]. Sphingomyelinases catalyze the hydrolysis of sphingomyelin to generate ceramide [reviewed in 70 and 71] which is a central molecule in modulating membrane biophysical properties and involved in various cellular process, such as apoptosis or inflammation, as well as several pathologies and diseases [48,65,69,89,90]. The acid sphingomyelinase/ceramide system, which has been shown as a crucial factor in the internalization and killing of various pathogens [45,46,91–96], modulates both the proinflammatory response and the state of mycobacteria in macrophages [97–102]. Our measurements of acid sphingomyelinase activities in macrophages revealed an activation of the enzyme in both, Wt- and Caveolin-1 deficient cells, during infection with BCG. However, Caveolin-1 deficient macrophages showed a higher activity of the acid sphingomyelinase, both basally and upon infection. In accordance, the generation of ceramide was increased after systemic infection for 3 weeks in the livers of Caveolin-1 deficient mice. Ceramide levels were higher in the livers of Caveolin-1 deficient mice compared to the livers of Wt mice. Finally, the level of sphingomyelin in Wt livers was

decreased after 1 and 3 weeks of infection. In summary, this resulted in a strong decrease of sphingomyelin/ceramide ratio in Caveolin-1 deficient mice upon infection with BCG. These data suggest a regulation of the acid sphingomyelinase (Asm)/ceramide system by caveolin-1, but the exact function of the acid sphingomyelinase in Caveolin-1 deficient cells remains to be determined.

Our *in vitro* studies demonstrated that Caveolin-1 deficient macrophages undergo more apoptosis 24 h after BCG infection compared to Wt cells (see Fig. 4A). Further, we show a higher expression of Bax and Caspase 9, but not Caspase 3 in macrophages and in livers of Caveolin-1 deficient mice after 1 week compared to Wt mice suggesting induction of intrinsic apoptosis in Caveolin-1 deficient cells and mice upon BCG infection. Mycobacterial infections trigger apoptosis via the extrinsic or the intrinsic pathway [103–105]. It needs to be determined whether the stronger induction of cell death in Caveolin-1 deficient cells depends on the stronger activation of the acid sphingomyelinase in these cells or whether other mechanisms mediate cell death upon BCG infection of Caveolin-1 deficient cells. A meaningful future approach to link these events, would be to cross Caveolin-1 deficient mice with acid sphingomyelinase-deficient mice and determine apoptosis upon BCG infection.

It has been described that BCG infection of murine macrophages effectively induces apoptosis by stimulation of Caspases 12, 9 and 3 thereby controlling intracellular bacteria. The infection induces an activation of interferon regulatory factor 3 (IRF3) and cytoplasmic Bax, leading to mitochondrial damage [62]. Bax is widely recognized as the most representative proapoptotic protein of the Bcl-2 family proteins and its localization and control on mitochondria are essential for the intrinsic pathway of apoptosis [106]. Several research groups also demonstrated Caspase 3 independent death pathways in mycobacterial infections. For example, IL-32γ induces death of *Mycobacterium tuberculosis*-infected macrophages through other mechanisms including those mediated by Caspase 1 and lysosomal cathepsins, thereby contributing to control of infection [107,108]. In addition, in response to apoptotic stimuli, mitochondria can also release Caspase-independent cell death effectors such as apoptosis-inducing factor (AIF) and Endonuclease G [109]. Another report describes, that apoptosis of macrophage upon BCG infection is independent of Caspase 3, 8 or 9 activation, but accompanied by translocation of apoptosis-inducing factor (AIF) [110]. Our research revealed no remarkable expression of apoptosis-inducing factor (AIF) in bone marrow-derived macrophages (not shown), suggesting, that at least mitochondrial protein AIF does not play a role in our model; Future studies on other mechanisms of Caspase 3 independent apoptosis, such as involvement of caspase-1, interferon regulatory factor 3 (IRF3), IL-32γ or various cathepsins could provide further insights into the nature of BCG-induced apoptosis in macrophages. We restricted ourselves to the measurement of cathepsin D (CTSD), which was induced independently of Caveolin-1 in our infection model. Although apoptosis is widely considered as host defense mechanism against bacterial infections, thus protecting the host from disease [reviewed in 111], it has been described, that apoptosis could also be disease-promoting if it eliminates key host defense cells, facilitates penetration of epithelial barriers, or spreads infection through efferocytosis [75,112]. Besides, several mycobacterial species, including BCG, *Mycobacterium tuberculosis* and *Mycobacterium avium* release distinct membrane vesicles containing lipids and proteins that subvert host immune response in a Toll-like receptor 2-dependent manner [113, 114].

A recent publication demonstrated differences in death mode in *M. tuberculosis*-infected murine macrophages, dependent on bacteria-to-host cell ratio (multiplicity of infection, MOI). The primary death mode, using high doses of infection (MOI ≥25:1) was apoptosis, based on nuclear morphology, although the apoptotic cells progressed rapidly to necrosis. The authors concluded that the presence of high numbers of intracellular bacteria triggers a macrophage cell death pathway that could promote the extracellular spread of infection and contribute to the formation of necrotic lesions in tuberculosis [115]. We used both, high multiplicity of infection (MOI) for detection of killing (CFU) and cell death (TUNEL) in macrophages (MOI 50:1) and low multiplicity of infection (MOI) for Western blots to measure apoptotic markers (MOI 10:1). For systemic infection of mice, we injected 1×10^7 bacteria, which represents a physiological dose. Based on literature reviews, we cannot rule out that our results represent a combination of apoptosis and necrosis, thus explaining the absence of Caspase-3 activation.

The results of the present work on the role of Caveolin-1 in autophagy upon BCG infection, revealed no notable involvement of this process in infection. It seems, that BCG could induce the autophagy pathway PI3K-AKT-mTOR and stimulate pBeclin, p62 and LC3B in Wt and Caveolin-1 deficient mice and macrophages in a more or less similar way upon mycobacterial infection.

5. Conclusions

Our studies demonstrate that Caveolin-1 is involved in infection of mice and murine macrophages with *Mycobacterium bovis* Bacillus Calmette-Guérin (BCG) by controlling acid sphingomyelinase (Asm) dependent ceramide production, apoptosis and inflammatory host responses. The deficiency of caveolin-1 leads to moderate higher bacterial burdens in the early phase of infection in livers of Caveolin-1 deficient mice and macrophages. These clues might be important in the fight against tuberculosis.

Data availability statement

All data are available upon request from the authors. Authors confirm that all data are included in the manuscript.

Funding

The study was supported by DFG grants GR 1697/2-1 and 2-2 to HG, GRK 2098 to HG, Gu 335/35-2 and Gu 335/38-1 to EG, and GRK 2581 to BK.

CRediT authorship contribution statement

Yuqing Wu: Writing – review & editing, Writing – original draft, Validation, Software, Methodology, Investigation, Formal analysis, Data curation, Conceptualization. **Andrea Riehle:** Methodology, Investigation, Data curation. **Barbara Pollmeier:** Methodology, Investigation, Data curation. **Stephanie Kadow:** Methodology, Investigation, Data curation. **Fabian Schumacher:** Methodology, Investigation, Data curation. **Marek Drab:** Resources, Methodology. **Burkhard Kleuser:** Methodology, Investigation, Data curation. **Erich Gulbins:** Writing – review & editing, Writing – original draft, Supervision, Funding acquisition, Conceptualization. **Heike Grassmé:** Writing – review & editing, Writing – original draft, Visualization, Validation, Supervision, Methodology, Investigation, Funding acquisition, Formal analysis, Data curation, Conceptualization.

Declaration of competing interest

The authors declare that the research was conducted in the absence of any commercial or financial relationships that could be constructed as a potential conflict of interest.

Acknowledgements

We thank Simone Keitsch, Melanie Kramer, Claudine Kühn and Matthias Soddemann for excellent technical support and our central animal unit for excellent care for the mice. We are grateful to Prof. Dr. Verena Jendrossek and Prof. Dr. Diana Klein from the Institute of Cell Biology, University of Duisburg-Essen, for providing us with mice to set

up our own breeding. Further, we thank Daniel Herrmann for excellent technical assistance with the LC-MS/MS measurements. We acknowledge support by the Open Access Publication Fund of the University of Duisburg-Essen.

Abbreviations

BCG, *Mycobacterium bovis* Bacillus Calmette-Guérin; Cav-1, Caveolin-1; BMDMs, bone marrow-derived macrophages; CFU, colony forming units; Wt, Wildtype.

Appendix A. Supplementary data

Supplementary data to this article can be found online at https://doi.org/10.1016/j.tube.2024.102493.

References

[1] WHO global tuberculosis report 2017. 2018. http://www.who.int/tb/publications/global_report/en/.
[2] Dheda K, Schwander SK, Zhu B, van Zyl-Smit RN, Zhang Y. The immunology of tuberculosis: from bench to bedside. Respiratory 2010;15:433–50. https://doi.org/10.1111/j.1440-1843.2010.01739.x.
[3] Bagcchi S. WHO's global tuberculosis report 2022. The Lancet Microbe 2023;4(1):E20. https://doi.org/10.1016/S2666-5247(22)00359-7.
[4] Barrios-Payán J, Saqui-Salces M, Jeyanathan M, Alcántara-Vazquez A, Castañon-Arreola M, Rook G, Hernandez-Pando R. Extrapulmonary locations of Mycobacterium tuberculosis DNA during latent infection. J Infect Dis 2012;206(15):1194–205. https://doi.org/10.1093/infdis/jis381.
[5] Qian X, Nguyen DT, Lyu J, Albers AE, Bi X, Graviss EA. Risk factors for extrapulmonary dissemination of tuberculosis and associated mortality during treatment for extrapulmonary tuberculosis. Emerg Microb Infect 2018;7(1):1–14. https://doi.org/10.1038/s41426-018-0106-1.
[6] Waters WR, Palmer MV. Mycobacterium bovis infection of cattle and white-tailed deer: translational research of relevance to human tuberculosis. ILAR J 2015;56(1):26–43. https://doi.org/10.1093/ilar/ilv001.
[7] Garnier T, Eiglmeier K, Camus JC, Medina N, Mansoor H, Pryor M, Duthoy S, Grondin S, Lacroix C, Monsempe C, Simon S, Harris B, Atkin R, Doggett J, Mayes R, Keating L, Wheeler PR, Parkhill J, Barrell BG, Cole ST, Gordon SV, Hewinson RG. The complete genome sequence of Mycobacterium bovis. Proc. Natl. Acad. Sci. U S A. Jun 24 2003;100(13):7877–82. https://doi.org/10.1073/pnas.1130426100.
[8] Oh YK, Straubinger RM. Intracellular fate of Mycobacterium avium: use of dual-label spectrofluorometry to investigate the influence of bacterial viability and opsonization on phagosomal pH and phagosome-lysosome interaction. Infect Immun 1996;64:319–25. https://doi.org/10.1128/iai.64.1.319-325.1996.
[9] Via LE, Deretic D, Ulmer RJ, Hibler NS, Huber LA, Deretic V. Arrest of mycobacterial phagosome maturation is caused by a block in vesicle fusion between stages controlled by rab 5 and rab 7. J. Biol. Chem. May 16 1997;272(20):13326–31. https://doi.org/10.1074/jbc.272.20.13326.
[10] Russell DG. Who puts the tubercle in tuberculosis? Nat. Rev. Microbiol. Jan 2007;5(1):39–47. https://doi.org/10.1038/nrmicro1538.
[11] Wang J, Li BX, Ge PP, Li J, Wang Q, Gao GF, Qiu XB, Liu CH. Mycobacterium tuberculosis suppresses innate immunity by coopting the host ubiquitin system. Nat. Immunol. Mar 2015;16(3):237–45. https://doi.org/10.1038/ni.3096.
[12] Aldwell FE, Wedlock DN, Buddle BM. Bacterial metabolism, cytokine mRNA transcription and viability of bovine alveolar macrophages infected with Mycobacterium bovis BCG or virulent M. bovis. Immunol Cell Biol 1996;74(1):45–51. https://doi.org/10.1038/icb.1996.6.
[13] Murata M, Peranen J, Schreiner R, Wieland F, Kurzchalia TV, Simons K. VIP21/caveolin is a cholesterol-binding protein. Proc Natl Acad Sci USA 1995;92:10339–43. https://doi.org/10.1073/pnas.92.22.10339.
[14] Schnitzer JE, McIntosh DP, Dvorak AM, Liu J, Oh P. Separation of caveolae from associated microdomains of GPI-anchored proteins. Science 1995;269:1435–9. https://doi.org/10.1126/science.7660128.
[15] Okamoto T, Schlegel A, Scherer PE, Lisanti MP. Caveolins, a family of scaffolding proteins for organizing "preassembled signaling complexes" at the plasma membrane. J Biol Chem 1998;272:5419–22. https://doi.org/10.1074/jbc.273.10.5419.
[16] Mineo C, James GL, Smart EJ, Anderson RG. Localization of epidermal growth factor-stimulated Ras/Raf-1 interaction to caveolae membrane. J Biol Chem 1996;271:11930–5. https://doi.org/10.1074/jbc.271.20.11930.
[17] Anderson RG. The caveolae membrane system. Annu Rev Biochem 1998;67:199–225. https://doi.org/10.1146/annurev.biochem.67.1.199.
[18] Cohen AW, Hnasko R, Schubert W, Lisanti MP. Role of caveolae and caveolins in health and disease. Physiol Rev 2004;84:1341–79. https://doi.org/10.1152/physrev.00046.2003.
[19] Anderson RG, Kamen BA, Rothberg KG, Lacey SW. Potocytosis: sequestration and transport of small molecules by caveolae. Science 1992;255:410–1. https://doi.org/10.1126/science.1310359.
[20] Smart EJ, Graf GA, McNiven MA, Sessa WC, Engelman JA, Scherer PE, Okamoto T, Lisanti MP. Caveolins, liquid-ordered domains, and signal transduction. Mol Cell Biol 1999;19:7289–304. https://doi.org/10.1128/mcb.19.11.7289.
[21] Patel HH, Murray F, Insel PA. Caveolae as organizers of pharmacologically relevant signal transduction molecules. Annu Rev Pharmacol Toxicol 2008;48:359–91. https://doi.org/10.1146/annurev.pharmtox.48.121506.124841.
[22] Zundel W, Swiersz LM, Giaccia A. Caveolin 1-mediated regulation of receptor tyrosine kinase-associated phosphatidylinositol 3-kinase activity by ceramide. Mol Cell Biol 2000;20:1507–14. https://doi.org/10.1128/mcb.20.5.1507-1514.2000.
[23] Liu J, Lee P, Galbiati F, Kitsis RN, Lisanti MP. Caveolin-1 expression sensitizes fibroblastic and epithelial cells to apoptotic stimulation. Am. J. Physiol. Cell. Physiol. Apr 2001;280(4):C823–35. https://doi.org/10.1152/ajpcell.2001.280.4.c823.
[24] Wu P, Qi B, Zhu H, Zheng Y, Li F, Chen J. Suppression of staurosporine-mediated apoptosis in Hs578T breast cells through inhibition of neutral-sphingomyelinase by caveolin-1. Cancer Lett 2007;256(1):64–72. https://doi.org/10.1016/j.canlet.2007.05.007.
[25] Meyer C, Liu Y, Kaul A, Peipe I, Dooley S. Caveolin-1 abrogates TGF-β mediated hepatocyte apoptosis. Cell Death Dis 2013;4(1):e466. https://doi.org/10.1038/cddis.2012.204.
[26] Xu L, Wang L, Wen Z, Wu L, Jiang Y, Yang L, Xiao L, Xie Y, Ma M, Zhu W, Ye R, Liu X. Caveolin-1 is a checkpoint regulator in hypoxia-induced astrocyte apoptosis via Ras/Raf/ERK pathway. Am J Physiol Cell Physiol. Jun 1 2016;310(11):C903–10. https://doi.org/10.1152/ajpcell.00309.2015.
[27] Ketteler J, Wittka A, Leonetti D, Roy VV, Estephan H, Maier P, Reis H, Herskind C, Jendrossek V, Paris F, Klein D. Caveolin-1 regulates the ASMase/ceramide-mediated radiation response of endothelial cells in the context of tumor-stroma interactions. Cell Death Dis 2020;11(4):228. https://doi.org/10.1038/s41419-020-2418-z.
[28] Gadjeva M, Paradis-Bleau C, Priebe GP, Fichorova R, Pier GB. Caveolin-1 modifies the immunity to Pseudomonas aeruginosa. J Immunol 2010;184:296–302. https://doi.org/10.4049/jimmunol.0900604.
[29] Medina FA, de Almeida CJ, Dew E, Li J, Bonuccelli G, Williams TM, Cohen AW, Pestell RG, Frank PG, Tanowitz HB, Lisanti MP. Caveolin-1-deficient mice show defects in innate immunity and inflammatory immune response during Salmonella enterica serovar Typhimurium infection. Infect. Immun. Dec 2006;74(12):6665–74. https://doi.org/10.1128/iai.00949-06.
[30] Guo Q, Shen N, Yuan K, Li J, Wu H, Zeng Y, Fox J, Bansal AK, Singh BB, Gao H, Wu M. Caveolin-1 plays a critical role in host immunity against Klebsiella pneumoniae by regulating STAT5 and Akt activity. Eur. J. Immunol. Jun 2012;42(6):1500–11. https://doi.org/10.1002/eji.201142051.
[31] Pietiäinen V, Marjomäki V, Upla P, Pelkmans L, Helenius A, Hyypiä T. Echovirus 1 endocytosis into caveosomes requires lipid rafts, dynamin II, and signaling events. Mol Biol Cell 2004;15:4911–25. https://doi.org/10.1091/mbc.e04-01-0070.
[32] Werling D, Hope JC, Chaplin P, Collins RA, Taylor G, Howard CJ. Involvement of caveolae in the uptake of respiratory syncytial virus antigen by dendritic cells. J Leukoc Biol 1999;66:50–8. https://doi.org/10.1002/jlb.66.1.50.
[33] Chen Y, Norkin LC. Extracellular simian virus 40 transmits a signal that promotes virus enclosure within caveolae. Exp Cell Res 1999;246:83–90. https://doi.org/10.1006/excr.1998.4301.
[34] Mergia A. The role of Caveolin 1 in HIV infection and pathogenesis. Viruses 2017;9:129. https://doi.org/10.3390/v9060129.
[35] Shin JS, Abraham SN. Co-option of endocytic functions of cellular caveolae by pathogens. Immunology 2001;102:2–7. https://doi.org/10.1046/j.1365-2567.2001.01173.x.
[36] Kaul D, Anand PK, Verma I. Cholesterol-sensor initiates M. tuberculosis entry into human macrophages. Mol. Cell. Biochem. Mar 2004;258(1–2):219–22. https://doi.org/10.1023/b:mcbi.0000012851.42642.be.
[37] Maldonado-García G, Chico-Ortiz M, Lopez-Marin LM, Sánchez-García FJ. High-polarity Mycobacterium avium-derived lipids interact with murine macrophage lipid rafts. Scand. J. Immunol. Nov 2004;60(5):463–70. https://doi.org/10.1111/j.0300-9475.2004.01511.x.
[38] Peyron P, Bordier C, N'Diaye EN, Maridonneau-Parini I. Non-opsonic phagocytosis of Mycobacterium kansasii by human neutrophils depends on cholesterol and is mediated by CR3 associated with glycosylphosphatidylinositol-anchored proteins. J Immunol 2000;165(9):5186–91. https://doi.org/10.4049/jimmunol.165.9.5186.
[39] Gatfield J, Pieters J. Essential role for cholesterol in entry of mycobacteria into macrophages. Science 2000;288(5471):1647–50. https://doi.org/10.1126/science.288.5471.1647.
[40] John V, Kotze LA, Ribechini E, Walzl G, Du Plessis N, Lutz MB. Caveolin-1 controls vesicular TLR2 expression, p38 signaling and T cell suppression in BCG infected murine monocytic myeloid-derived suppressor cells. Front Immunol 2019;10:2826. https://doi.org/10.3389/fimmu.2019.02826.
[41] Grassmé H, Jekle A, Riehle A, Schwarz H, Berger J, Sandhoff K, Kolesnick R, Gulbins E. CD95 signaling via ceramide-rich membrane rafts. J. Biol. Chem. Jun 8 2001;276(23):20589–96. https://doi.org/10.1074/jbc.m101207200.
[42] Grassmé H, Jendrossek V, Bock J, Riehle A, Gulbins E. Ceramide-rich membrane rafts mediate CD40 clustering. J. Immunol. Jan 1 2002;168(1):298–307. https://doi.org/10.4049/jimmunol.168.1.298.
[43] Nurminen TA, Holopainen Paavo JMH, Kinnunen KJ. Observation of topical catalysis by sphingomyelinase coupled to microspheres. J Am Chem Soc 2002;124(41):12129–34. https://doi.org/10.1021/ja017807r.

[44] Esen M, Schreiner B, Jendrossek V, Lang F, Fassbender K, Grassmé H, Gulbins E. Mechanisms of Staphylococcus aureus induced apoptosis of human endothelial cells. Apoptosis 2001;6:431–9. https://doi.org/10.1023/a:1012445925628.
[45] Grassmé H, Jendrossek V, Riehle A, von Kürthy G, Berger J, Schwarz H, Weller M, Kolesnick R, Gulbins E. Host defense against Pseudomonas aeruginosa requires ceramide-rich membrane rafts. Nat. Med. 2003;9:322–30. https://doi.org/10.1038/nm823.
[46] Grassmé H, Riehle A, Wilker B, Gulbins E. Rhinoviruses infect human epithelial cells via ceramide-enriched membrane platforms. J Biol Chem 2005;280:26256–62. https://doi.org/10.1074/jbc.m500835200.
[47] Drab M, Verkade P, Elger M, Kasper M, Lohn M, Lauterbach B, Menne J, Lindschau C, Mende F, Luft FC, Schedl A, Haller H, Kurzchalia TV. Loss of caveolae, vascular dysfunction, and pulmonary defects in caveolin-1 gene-disrupted mice. Science 2001;293(5539):2449–52. https://doi.org/10.1126/science.1062688.
[48] Zhang Y, Li X, Carpinteiro A, Gulbins E. Acid sphingomyelinase amplifies redox signaling in Pseudomonas aeruginosa-induced macrophage apoptosis. J Immunol 2008;181:4247–54. https://doi.org/10.4049/jimmunol.181.6.4247.
[49] Fazal N, Lammas DA, Raykundalia C, Bartlett R, Kumararatne DS. Effect of blocking TNF-alpha on intracellular BCG (Bacillus Calmette Guérin) growth in human monocyte-derived macrophages. FEMS Microbiol Immunol 1992;5:337–45. https://doi.org/10.1111/j.1574-6968.1992.tb05919.x.
[50] Humphreys IR, Stewart GR, Turner DJ, Patel J, Karamanou D, Snelgrove RJ, Young DB. A role for dendritic cells in the dissemination of mycobacterial infection. Microb Infect 2006;8:1339–46. https://doi.org/10.1016/j.micinf.2005.12.023.
[51] Mühle C, Kornhuber J. Assay to measure sphingomyelinase and ceramidase activities efficiently and safely. J Chromatogr 2017;20:137–44. https://doi.org/10.1016/j.chroma.2016.12.033.
[52] Gulbins A, Schumacher F, Becker KA, Wilker B, Soddemann M, Boldrin F, Müller CP, Edwards MJ, Goodman M, Caldwell CC, Kleuser B, Kornhuber J, Szabo I, Gulbins E. Antidepressants act by inducing autophagy controlled by sphingomyelin-ceramide. Mol. Psychiatry Dec 2018;23(12):2324–46. https://doi.org/10.1038/s41380-018-0090-9.
[53] Günther A, Hose M, Abberger H, Schumacher F, Veith Y, Kleuser B, Matuschewski K, Lang KS, Gulbins E, Buer J, Westendorf AM, Hansen W. The acid ceramidase/ceramide axis controls parasitemia in Plasmodium yoelii-infected mice by regulating erythropoiesis. Elife Sep 2022;12:e77975. https://doi.org/10.7554/elife.77975.
[54] Thandi RS, Tripathi D, Kumar R, Paidipally RP, Vankayalapati R. Kupffer cells restricts Mycobacterium tuberculosis growth better than alveolar macrophages. J Immunol 2018;1(1-Supplement). https://doi.org/10.4049/jimmunol.200.Supp.173.20.
[55] Beattie L, Sawtell A, Mann J, Frame TCM, Teal B, de Labastida Rivera F, Brown N, Walwyn-Brown K, Moore JWJ, MacDonald S, Lim EK, Dalton JE, Engwerda CR, MacDonald KP, Kaye PM. Bone marrow-derived and resident liver macrophages display unique transcriptomic signatures but similar biological functions. J Hepatol 2016;65:758–68. https://doi.org/10.1016/j.jhep.2016.05.037.
[56] Wu Y, Li C, Riehle A, Pollmeier B, Gulbins E, Grassmé H. Mycobacterial infection is promoted by neutral sphingomyelinase 2 regulating a signaling cascade leading to activation of β1-Integrin. Cell Physiol Biochem 2018;51(4):1815–29. https://doi.org/10.1159/000495683.
[57] Zhang W, Liu H. MAPK signal pathways in the regulation of cell proliferation in mammalian cells. Cell Res 2002;12:9–18. https://doi.org/10.1038/sj.cr.7290105.
[58] Gutierrez MG, Master SS, Singh SB, Taylor GA, Colombo MI, Deretic V. Autophagy is a defense mechanism inhibiting BCG and Mycobacterium tuberculosis survival in infected macrophages. Cell 2004;119(6):753–66. https://doi.org/10.1016/j.cell.2004.11.038.
[59] Kumar D, Nath L, Kamal MA, Varshney A, Jain A, Singh S, Rao KV. Genome-wide analysis of the host intracellular network that regulates survival of Mycobacterium tuberculosis. Cell Mar 5 2010;140(5):731–43. https://doi.org/10.1016/j.cell.2010.02.012.
[60] Li C, Peng H, Japtok L, Seitz A, Riehle A, Wilker B, Soddemann M, Kleuser B, Edwards M, Lammas D, Zhang Y, Gulbins E, Grassmé H. Inhibition of neutral sphingomyelinase protects mice against systemic tuberculosis. Front Biosci 2016;8:311–25. https://doi.org/10.2741/e769.
[61] Zhang Q, Sun J, Wang Y, He W, Wang L, Zheng Y, Wu J, Zhang Y, Jiang X. Antimycobacterial and anti-inflammatory mechanisms of Baicalin via induced autophagy in macrophages infected with Mycobacterium tuberculosis. Front. Microbiol. Nov 2017;2(8). https://doi.org/10.3389/fmicb.2017.02142.
[62] Cui Y, Zhao D, Sreevatsan S, Liu C, Yang W, Song Z, Yang L, Barrow P, Zhou X. Mycobacterium bovis induces endoplasmic reticulum stress mediated-apoptosis by activating IRF3 in a murine macrophage cell line. Front. Cell. Infect. Microbiol. Dec 2016;12(6):182. https://doi.org/10.3389/fcimb.2016.00182.
[63] Li P, Zhou L, Zhao T, Liu X, Zhang P, Liu Y, Zheng X, Li Q. Caspase-9: structure, mechanisms and clinical application. Oncotarget 2017;8(14):23996–4008. https://doi.org/10.18632/oncotarget.15098.
[64] Cifone MG, De Maria R, Roncaioli P, Rippo MR, Azuma M, Lanier LL, Santoni A, Testi R. Apoptotic signaling through CD95 (Fas/Apo-1) activates an acidic sphingomyelinase. J Exp Med 1994;180(4):1547–52. https://doi.org/10.1084/jem.180.4.1547.
[65] Gulbins E, Bissonnette R, Mahboubi A, Martin S, Nishioka W, Brunner T, Baier G, Baier-Bitterlich G, Byrd C, Lang F, Kolesnick R, Altmann A, Green D. FAS-induced apoptosis is mediated via a ceramide-initiated RAS signaling pathway. Immunity Apr 1995;2(4):341–51. https://doi.org/10.1016/1074-7613(95)90142-6.
[66] Brenner B, Ferlinz K, Grassmé H, Weller M, Koppenhoefer U, Dichgans J, Sandhoff K, Lang F, Gulbins E. Fas/CD95/Apo-I activates the acidic sphingomyelinase via caspases. Cell Death Differ. Jan 1998;5(1):29–37. https://doi.org/10.1038/sj.cdd.4400307.
[67] Kirschnek S, Paris F, Weller M, Grassmé H, Ferlinz K, Riehle A, Fuks Z, Kolesnick R, Gulbins E. CD95-mediated apoptosis in vivo involves acid sphingomyelinase. J Biol Chem 2000;275(35):27316–23. https://doi.org/10.1016/S0021-9258(19)61513-9.
[68] Gulbins E, Kolesnick R. Acid sphingomyelinase-derived ceramide signaling in apoptosis. Subcell Biochem 2002;36:229–44. https://doi.org/10.1007/0-306-47931-1_12.
[69] Zhao M, Pan W, Shi RZ, Bai YP, You BY, Zhang K, Fu QM, Schuchman EH, He XX, Zhang GG. Acid sphingomyelinase mediates oxidized-LDL induced apoptosis in macrophage via endoplasmic reticulum stress. J. Atheroscler. Thromb. Sep 1 2016;23(9):1111–25. https://doi.org/10.5551/jat.32383.
[70] Schuchman EH, Wasserstein MP. Types A and B niemann-pick disease. Best Pract. Res. Clin. Endocrinol. Metab. Mar 2015;29(2):237–47. https://doi.org/10.1016/j.beem.2014.10.002.
[71] Kornhuber J, Rhein C, Müller CP, Mühle C. Secretory sphingomyelinase in health and disease. Biol. Chem. Jun 2015;396(6–7):707–36. https://doi.org/10.1515/hsz-2015-0109.
[72] Tani M, Ito M, Igarashi Y. Ceramide/sphingosine/sphingosine 1-phosphate metabolism on the cell surface and in the extracellular space. Cell. Signal. Feb 2007;19(2):229–37. https://doi.org/10.1016/j.cellsig.2006.07.001.
[73] Flesch IEA, Kaufmann SHE. Role of cytokines in tuberculosis. Immunobiology 1993;189(3–4):316–39. https://doi.org/10.1016/S0171-2985(11)80364-5.
[74] Domingo-Gonzalez R, Prince O, Cooper A, Khader SA. Cytokines and chemokines in Mycobacterium tuberculosis infection. Microbiol. Spectr. Oct 2016;4(5). https://doi.org/10.1128/microbiolspec.tbtb2-0018-2016.
[75] Davis JM, Ramakrishnan L. The role of the granuloma in expansion and dissemination of early tuberculous infection. Cell 2009;136:37–49. https://doi.org/10.1016/j.cell.2008.11.014.
[76] Cronan MR, Beerman RW, Rosenberg AF, Saelens JW, Johnson MG, Oehlers SH, Sisk DM, Jurcic Smith KL, Medvitz NA, Miller SE, Trinh LA, Fraser SE, Madden JF, Turner J, Stout JE, Lee S, Tobin DM. Macrophage epithelial reprogramming underlies Mycobacterial granuloma formation and promotes infection. Immunity 2016;45(4):861–76. https://doi.org/10.1016/j.immuni.2016.09.014.
[77] Hernández-Pando R, Orozcoe H, Sampieri A, Pavón L, Velasquillo C, Larriva-Sahd J, Alcocer JM, Madrid MV. Correlation between the kinetics of Th1, Th2 cells and pathology in a murine model of experimental pulmonary tuberculosis. Immunology Sep 1996;89(1):26–33. https://pubmed.ncbi.nlm.nih.gov/8911136.
[78] Chakravarty SD, Xu J, Lu B, Gerard C, Flynn J, Chan J. The chemokine receptor CXCR3 attenuates the control of chronic Mycobacterium tuberculosis infection in BALB/c mice. J Immunol 2007;1(3):1723–35. https://doi.org/10.4049/jimmunol.178.3.1723.
[79] Hernandez-Pando R, Orozco H, Arriaga K, Sampieri A, Larriva-Sahd J, Madrid-Marina V. Analysis of the local kinetics and localization of interleukin-1 alpha, tumour necrosis factor-alpha and transforming growth factor-beta, during the course of experimental pulmonary tuberculosis. Immunology Apr 1997;90(4):607–17. https://doi.org/10.1046/j.1365-2567.1997.00193.x.
[80] Dambuza I, Allie N, Fick L, Johnston N, Fremond C, Mitchell J, Quesniaux VF, Ryffel B, Jacobs M. Efficacy of membrane TNF mediated host resistance is dependent on mycobacterial virulence. Tuberculosis (Edinb.) May 2008;88(3):221–34. https://doi.org/10.1016/j.tube.2007.08.011.
[81] Garrean S, Gao XP, Brovkovych V, Shimizu J, Zhao YY, Vogel SM, Malik AB. Caveolin-1 regulates NF-kappaB activation and lung inflammatory response to sepsis induced by lipopolysaccharide. J Immunol 2006;177(7):4853–60. https://doi.org/10.4049/jimmunol.177.7.4853.
[82] Reljic R, Stylianou E, Balu S, Ma JK. Cytokine interactions that determine the outcome of Mycobacterial infection of macrophages. Cytokine Jul 2010;51(1):42–6. https://doi.org/10.1016/j.cyto.2010.04.005.
[83] Goldberg MF, Saini NK, Porcelli SA. Evasion of innate and adaptive immunity by Mycobacterium tuberculosis. Microbiol. Spectr. Oct 2014;2(5). https://doi.org/10.1128/microbiolspec.MGM2-0005-2013.
[84] Blanc L, Gilleron M, Prandi J, Song OR, Jang MS, Gicquel B, Drocourt D, Neyrolles O, Brodin P, Tiraby G, Vercellone A, Nigou J. Mycobacterium tuberculosis inhibits human innate immune responses via the production of TLR2 antagonist glycolipids. Proc Natl Acad Sci USA 2017;17(42):11205–10. https://doi.org/10.1073/pnas.1707840114.
[85] Zhai W, Wu F, Zhang Y, Fu Y, Liu Z. The immune escape mechanisms of Mycobacterium tuberculosis. Int. J. Mol. Sci. Jan 15 2019;20(2):340. https://doi.org/10.3390/ijms20020340.
[86] Rastogi S, Ellinwood S, Augenstreich J, Mayer-Barber KD, Briken V. Mycobacterium tuberculosis inhibits the NLRP3 inflammasome activation via its phosphokinase PknF. PLoS Pathog. Jul 29 2021;17(7):e1009712. https://doi.org/10.1371/journal.ppat.1009712.
[87] Weiss G, Schaible UE. Macrophage defense mechanisms against intracellular bacteria. Immunol Rev 2015;264:182–203. https://doi.org/10.1111/imr.12266.
[88] Hannun YA, Obeid LM. Principles of bioactive lipid signalling: lessons from sphingolipids. Nat Rev Mol Cell Biol 2008;9:139–50. https://doi.org/10.1038/nrm2329.
[89] Schütze S, Potthoff K, Machleidt T, Berkovic D, Wiegmann K, Krönke M. TNF activates NF-kappa B by phosphatidylcholine-specific phospholipase C-induced "acidic" sphingomyelin breakdown. Cell 1992;71:765–76. https://doi.org/10.1016/0092-8674(92)90553-o.

[90] Falcone S, Perrotta C, De Palma C, Pisconti A, Sciorati C, Capobianco A, Rovere-Querini P, Manfredi AA, Clementi E. Activation of acid sphingomyelinase and its inhibition by the nitric oxide/cyclic guanosine 3',5'-monophosphate pathway: key events in Escherichia coli-elicited apoptosis of dendritic cells. J Immunol 2004;173:4452–63. https://doi.org/10.4049/jimmunol.173.7.4452.

[91] Grassmé H, Gulbins E, Brenner B, Ferlinz K, Sandhoff K, Harzer K, Lang F, Meyer TF. Acidic sphingomyelinase mediates entry of N. gonorrhoeae into nonphagocytic cells. Cell 1997;91:605–15. https://doi.org/10.1016/s0092-8674(00)80448-1.

[92] Hedlund M, Duan RD, Nilsson A, Svanborg C. Sphingomyelin, glycosphingolipids and ceramide signalling in cells exposed to P-fimbriated Escherichia coli. Mol Microbiol 1998;29:1297–306. https://doi.org/10.1046/j.1365-2958.1998.01017.x.

[93] Hauck CR, Grassmé H, Bock J, Jendrossek V, Ferlinz K, Meyer TF, Gulbins E. Acid sphingomyelinase is involved in CEACAM receptor-mediated phagocytosis of Neisseria gonorrhoeae. FEBS Lett 2000;478:260–6. https://doi.org/10.1016/s0014-5793(00)01851-2.

[94] Utermöhlen O, Karow U, Lohler J, Krönke M. Severe impairment in early host defense against Listeria monocytogenes in mice deficient in acid sphingomyelinase. J Immunol 2003;170:2621–8. https://doi.org/10.4049/jimmunol.170.5.2621.

[95] Gassert E, Avota E, Harms H, Krohne G, Gulbins E, Schneider-Schaulies S. Induction of membrane ceramides: a novel strategy to interfere with T lymphocyte cytoskeletal reorganisation in viral immunosuppression. PLoS Pathog 2009;5:e1000623. https://doi.org/10.1371/journal.ppat.1000623.

[96] Peng H, Li C, Kadow S, Henry BD, Steinmann J, Becker KA, Riehle A, Beckmann N, Wilker B, Li PL, Pritts T, Edwards MJ, Zhang Y, Gulbins E, Grassmé H. Acid sphingomyelinase inhibition protects mice from lung edema and lethal Staphylococcus aureus sepsis. J. Mol. Med. (Berl.) Jun 2015;93(6):675–89. https://doi.org/10.1007/s00109-014-1246-y.

[97] Anes E, Kühnel MP, Bos E, Moniz-Péreira J, Habermann A, Griffiths G. Selected lipids activate phagosome actin assembly and maturation resulting in killing of pathogenic mycobacteria. Nat Cell Biol 2003;5:793–802. https://doi.org/10.1038/ncb1036.

[98] Utermöhlen O, Herz J, Schramm M, Krönke M. Fusogenicity of membranes: the impact of acid sphingomyelinase on innate immune responses. Immunobiology 2008;213:307–14. https://doi.org/10.1016/j.imbio.2007.10.016.

[99] Wahe A, Kasmapour B, Schmaderer C, Liebl D, Sandhoff K, Nykjaer A, Griffiths G, Gutiérrez MG. Golgi-to-phagosome transport of acid sphingomyelinase and prosaposin is mediated by sortilin. J Cell Sci 2010;123:2502–11. https://doi.org/10.1242/jcs.067686.

[100] Roca FJ, Ramakrishnan L. TNF dually mediates resistance and susceptibility to mycobacteria via mitochondrial reactive oxygen species. Cell 2013;153:521–34. https://doi.org/10.1016/j.cell.2013.03.022.

[101] Vázquez CL, Rodgers A, Herbst S, Coade S, Gronow A, Guzman CA, Wilson MS, Kanzaki M, Nykjaer A, Gutierrez MG. The proneurotrophin receptor sortilin is required for Mycobacterium tuberculosis control by macrophages. Sci Rep 2016;6:1–13. https://doi.org/10.1038/srep29332.

[102] Wu Y, Li C, Peng H, Swaidan A, Riehle A, Pollmeier B, Zhang Y, Gulbins E, Grassmé H. Acid sphingomyelinase contributes to the control of mycobacterial infection via a signaling cascade leading from reactive oxygen species to cathepsin D. Cells 2020;9(11):2406. https://doi.org/10.3390/cells9112406.

[103] Molloy A, Laochumroonvorapong P, Kaplan G. Apoptosis, but not necrosis, of infected monocytes is coupled with killing of intracellular Bacillus Calmette-Guérin. J Exp Med 1994;180(4):1499–509. https://doi.org/10.1084/jem.180.4.1499.

[104] Duan L, Gan H, Arm J, Remold HG. Cytosolic phospholipase A2 participates with TNF-α in the induction of apoptosis of human macrophages infected with Mycobacterium tuberculosis H37Ra1. J Immunol 2001;166:7469–76. https://doi.org/10.4049/jimmunol.166.12.7469.

[105] Riendeau CJ, Kornfeld H. THP-1 cell apoptosis in response to mycobacterial infection. Infect Immun 2003;71:254–9. https://doi.org/10.1128/iai.71.1.254-259.2003.

[106] Lindsay J, Esposti MD, Gilmore AP. Bcl-2 proteins and mitochondria-specificity in membrane targeting for death. Biochim Biophys Acta. Apr 2011;1813(4):532–9. https://doi.org/10.1016/j.bbamcr.2010.10.017.

[107] Bai X, Kinney WH, Su WL, Bai A, Ovrutsky AR, Honda JR, Netea MG, Henao-Tamayo M, Ordway DJ, Dinarello CA, Chan ED. Caspase-3-independent apoptotic pathways contribute to interleukin-32γ-mediated control of Mycobacterium tuberculosis infection in THP-1 cells. BMC Microbiol 2015;21:15–39. https://doi.org/10.1186/s12866-015-0366-z.

[108] Li Z, Wang Y, Liu X, Xing X, Zhang Y. Interleukin-32ε induces caspase-independent apoptosis mediated by N-Myc interactor in macrophages infected with Mycobacterium tuberculosis. FEBS J. Feb 2019;286(3):572–83. https://doi.org/10.1111/febs.14717.

[109] Cregan SP, Dawson VL, Slack RS. Role of AIF in caspase-dependent and caspase-independent cell death. Oncogene Apr 2004;12(16):2785–96. https://doi.org/10.1038/sj.onc.1207517.

[110] Vega-Manriquez X, López-Vidal Y, Moran J, Adams LG, Gutiérrez-Pabello JA. Apoptosis-inducing factor participation in bovine macrophage Mycobacterium bovis-induced caspase-independent cell death. Infect. Immun. Mar 2007;75(3):1223–8. https://doi.org/10.1128/iai.01047-06.

[111] Moraco AH, Kornfeld H. Cell death and autophagy in tuberculosis. Semin. Immunol. Dec 2014;26(6):497–511. https://doi.org/10.1016/j.smim.2014.10.001.

[112] Zychlinsky A. Programmed cell death in infectious diseases. Trends Microbiol. Jun 1993;1(3):114–7. https://doi.org/10.1016/0966-842x(93)90118-b.

[113] Prados-Rosales R, Baena A, Martinez LR, Luque-Garcia J, Kalscheuer R, Veeraraghavan U, Camara C, Nosanchuk JD, Besra GS, Chen B, Jimenez J, Glatman-Freedman A, Jacobs Jr WR, Porcelli SA, Casadevall A. Mycobacteria release active membrane vesicles that modulate immune responses in a TLR2-dependent manner in mice. J. Clin. Invest. Apr 2011;121(4):1471–83. https://doi.org/10.1172/jci44261.

[114] Early J, Fischer K, Bermudez LE. Mycobacterium avium uses apoptotic macrophages as tools for spreading. Microb. Pathog. Feb 2011;50(2):132–9. https://doi.org/10.1016/j.micpath.2010.12.004.

[115] Lee J, Remold HG, Ieong MH. Macrophage apoptosis in response to high intracellular burden of Mycobacterium tuberculosis is mediated by a novel caspase-independent pathway. J Immunol 2006;176:4267–74. https://doi.org/10.4049/jimmunol.176.7.4267.